ELSEVIER

Journal of Hepatology 47 (2007) 546–555

Journal of Hepatology

www.elsevier.com/locate/jhep

Abrogation of constitutive STAT3 activity sensitizes human hepatoma cells to TRAIL-mediated apoptosis☆

Mariko Kusaba, Kazuhiko Nakao*, Takashi Goto, Daisuke Nishimura, Hiroshi Kawashimo, Hidetaka Shibata, Yasuhide Motoyoshi, Naota Taura, Tatsuki Ichikawa, Keisuke Hamasaki, Katsumi Eguchi

First Department of Internal Medicine, Nagasaki University School of Medicine, 1-7-1, Sakamoto, Nagasaki 852-8501, Japan

***Background/Aims*: Signal transducer and activator of transcription 3 (STAT3) is constitutively activated and regulates cell growth and survival of various cancer cells. We investigated the anti-tumor effect of AG490, a Janus kinase 2 specific inhibitor, in human hepatoma cells.**

***Methods*: Effects of AG490 on STAT3 activation, on cell-growth and survival, and on the expression of cell-cycle- and apoptosis-related proteins were evaluated in Huh-1, Huh-7, HepG2 and Hep3B cells. Next, whether AG490 renders hepatoma cells susceptible to tumor necrosis factor-related apoptosis-inducing ligand (TRAIL) was examined *in vitro* and *in vivo*.**

***Results*: Constitutively activated STAT3 through tyrosine phosphorylation was detected in all hepatoma cells. AG490 inhibited the phosphorylation of STAT3 and its activity. AG490 induced cell cycle arrest in Huh-1, Huh-7 and HepG2 through cyclin D1 downregulation, and induced marked apoptosis in Hep3B. AG490 downregulated at least one of the anti-apoptotic proteins, Bcl-xL, survivin or XIAP in all hepatoma cells. AG490 sensitized Huh-1, Huh-7 and HepG2 to TRAIL-induced apoptosis *in vitro*. Intraperitoneal injection of AG490, the combination of AG490 and TRAIL more greatly, repressed the growth of subcutaneous Huh-7 tumors in athymic mice.**

***Conclusions*: Abrogation of constitutive activation of STAT3 by AG490 enhances the anti-tumor activity of TRAIL against human hepatoma cells.**

***Keywords*: STAT3; AG490; TRAIL; Hepatoma**

1. Introduction

Signal transducer and activator of transcription (STAT) proteins become activated by tyrosine phosphorylation in response to cytokines and growth factors, which typically occurs through cytokine receptor-associated kinases, the Janus kinase (JAK) family proteins [1]. Recent studies have demonstrated that constitutively activated STAT signaling, especially STAT3, contributes to oncogenesis [2,3]. In fact, constitutive activation of STAT3 has been observed in various cancer cells [2–8], suggesting that STAT3 plays a crucial role in the regulation of cell proliferation and survival in cancer. Furthermore, abrogation of STAT3 signaling by

Received 1 December 2006; received in revised form 24 April 2007; accepted 26 April 2007; available online 6 June 2007
Associate Editor: K. Koike

☆ The authors who have taken part in this study declared that they have no relationship with the manufacturers of the materials involved either in the past or present and did not receive funding from the manufacturers to carry out their research. They did not receive funding from any source to carry out this study.

* Corresponding author. Tel.: +81 95 849 7261; fax: +81 95 849 7261.

E-mail address: kazuhiko@net.nagasaki-u.ac.jp (K. Nakao).

Abbreviations: JAK2, Janus kinase 2; SOCS, suppressor of cytokine signaling; STAT3, signal transducer and activator of transcription 3; TRAIL, tumor necrosis factor-related apoptosis-inducing ligand.

0168-8278/$32.00
doi:10.1016/j.jhep.2007.04.017

chemical inhibitors [9,10], a dominant negative STAT3 mutant [11,12], inhibitory phosphotyrosyl peptides [13], decoy oligonucleotides [14], antisense STAT3 oligonucleotides [15] has resulted in inhibition of cell proliferation and induction of apoptosis in various cancer cells [16].

Hepatitis B virus (HBV) and hepatitis C virus (HCV) are closely linked to the development of hepatocellular carcinoma (HCC) [17,18]. Recently, it has been reported that suppressor of cytokine signaling (SOCS)-1 and SOCS-3, negative regulators of the JAK2-STAT signaling pathway, are silenced by methylation in human hepatoma cell lines and HCC tissues, which leads to constitutive activation of STAT3 in these cells [19,20]. It was also reported that STATs including STAT3 were aberrantly activated in HCC tissues compared with surrounding normal liver tissues [21,22]. In addition, several studies have shown that HCV constitutively activates STAT3 through oxidative stress [23], and that the HCV core protein can activate STAT3, resulting in the cellular transformation [24]. Taken together, it is possible that the constitutive activation of STAT3 is involved in hepatocarcinogenesis.

Tumor necrosis factor (TNF)-related apoptosis-inducing ligand (TRAIL), a novel member of the TNF superfamily, is a promising candidate for cancer therapy since it preferentially induces apoptosis in various cancer cells with little or no effect on normal cells [25,26]. However, high concentrations of TRAIL are necessary to induce apoptosis in certain cancer cells, including human hepatoma cells [27]. Thus, combinations of TRAIL with several chemotherapeutic agents or radiation have been evaluated for rendering such cells susceptible to TRAIL, and some combinations have successfully enhanced TRAIL-mediated cancer cell death [27–29].

In the present study, we examined the status of STAT3 activation in human hepatoma cells and the effect of the JAK2 inhibitor, AG490, on STAT3 activation and on cell proliferation and survival. Furthermore, we have evaluated whether abrogation of STAT3 signaling by AG490 sensitizes hepatoma cells to TRAIL-induced apoptosis *in vitro* and combination of AG490 and TRAIL exhibits anti-tumor effect *in vivo*.

2. Materials and methods

2.1. Cell culture and reagents

The human hepatoma cell lines, Huh-1, HuH-7, HepG2 and Hep3B, were maintained in a chemically defined medium, IS-RPMI [30] containing 10% fetal bovine serum. Normal human hepatocytes (Hc cells) [31] were purchased from the Applied Cell Biology Research Institute (Kirkland, WA) and maintained in CS-C complete medium. A JAK-2 specific inhibitor, AG490, was purchased from Calbiochem (San Diego, CA). Recombinant human TRAIL was purchased from R&D systems (Minneapolis, MN). In some experiments, interleukin-6 (IL-6) (R&D systems), cell permeable STAT3 inhibitor peptide containing STAT3-SH2 domain-binding PY*LKTK where Y* represents phosphotyrosine (Calbiochem) [13], and DR4 and DR5-specific blocking chimera antibodies (DR4-chimera and DR5-chimera) (R&D systems) were added to the cell cultures.

2.2. Cell transfection and luciferase assay

The plasmids pTA-Luc (Clontech, Mountain View, CA) containing the minimal TA promoter and the firefly luciferase gene, pSTAT3-TA-Luc (Clontech), containing four copies of the binding sequence of STAT3 located upstream of pTA-Luc promoter, and pRL-CMV-Luc (Promega, Madison, WI) containing the CMV immediate early enhancer/promoter and the *Renilla* luciferase gene were used. Cells were grown in 24-well multiplates the day before transfection. Two hundred nanograms of pSTAT3-TA-Luc or pTA-Luc together with 10 ng pRL-CMV-Luc was transfected into the cells by the lipofection method. After 6 h incubation, the medium was replaced with fresh medium with or without IL-6 (20, 40 ng/ml), AG490 (25, 100 μM) or STAT3 inhibitor peptide (0.1, 0.5 mM), and the cells were incubated for 24 h. Luciferase activity was determined by a dual-luciferase reporter assay system and a TD-2020 luminometer (Promega).

2.3. Cell cycle analysis and detection of apoptosis

Cells were incubated with AG490 (100 μmol/L) and/or TRAIL (2 ng/ml) or vehicle alone (0.1% DMSO) for 24 h, fixed with 70% ethanol treated with RNase (100 μg/ml, Sigma Chemical Co., St. Louis, MO), and stained with propidium iodide (100 μg/ml, Sigma) for 30 min on ice. DNA content in the cells was analyzed by a flow cytometer (Epics XL; Beckman Coulter, Miami, FL). Apoptosis was also analyzed by ApoStrand™ ELISA apoptosis detection kit (Biomol International, PA) which detects the denatured DNA in apoptotic cells with a monoclonal antibody to single-stranded DNA.

2.4. Western blotting

Cells were lysed by addition of lysis buffer (50 mM Tris [pH 8.0], 150 mM NaCl, 0.1% SDS, 100 μg/ml PMSF, 1% NP40, 0.5% sodium deoxycholate and 1 mM sodium *o*-vanadate). Twenty micrograms of each lysate was electrophoresed on SDS–polyacrylamide gels and electrotransferred to nitrocellulose membranes, and incubated for 1 h in the presence of each of the following antibodies; mouse monoclonal anti-human phospho-(Y-705)-STAT3 (Cell Signaling, Beverly, MA), rabbit polyclonal anti-human STAT3, Bcl-xL, XIAP, survivin, cyclinD1 and Waf1/p21 (Cell Signaling), rabbit polyclonal anti-human Bax, CIAP-1 and CIAP-2 (Santa Cruz Biotechnology, Santa Cruz, CA), rabbit polyclonal anti-human FLIP (PharMingen, San Diego, CA), mouse monoclonal anti-human SOCS-1 and SOCS-3 (MBL, Nagoya, Japan), rabbit polyclonal anti-human DR4 and DR5 (Imgenex, San Diego, CA) and mouse monoclonal anti-human β-actin (Sigma) as an internal control. The membranes were washed and incubated with horseradish peroxidase-conjugated anti-rabbit IgG or anti-mouse IgG for 1 h. Immunoreactive bands were visualized by the ECL chemiluminescence system (Amersham Life Science, Buckinghamshire, UK).

2.4.1. RT-PCR

RT-PCR was performed using OneStep RT-PCR Kit (Qiagen, Valencia, CA) and Human TRAIL-R1/DR4 or TRAIL-R2/DR5 primer pairs (R&D Systems) to yield a 567-bp or 432 and 345-bp products, respectively. The amplification was performed for 30 cycles in a programmable DNA thermal cycler.

2.5. In vivo study

Five-week-old male BALB/c nu/nu athymic mice were purchased from Charles River Japan (Yokohama, Japan). Animal experiments were performed in accordance with institutional guidelines, and the study was approved by the Ethics Committee of Nagasaki University.

Huh-7 cells (3×10^6) were implanted subcutaneously into the right thigh of mice, when the tumor diameter reached 5 mm. AG490 (0.5 mg/mouse) and/or TRAIL (40 ng/mouse) was injected into the peritoneal space once a day for 13 days. As a control, 0.1 ml of vehicle (50% DMSO) was injected. Each group consisted of five mice. Tumor growth was monitored daily by measuring two perpendicular tumor diameters with a caliper, and tumor volume was calculated using a formula; (width^2 × length)/2. At the end of the study, tumors were resected from mice, weighted, and subjected to histopathological examination together with liver tissues.

2.6. Statistical analysis

Variable data were expressed as means ± SD. Differences between groups were examined for statistical significance using Student's *t* test.

3. Results

3.1. AG490 inhibits constitutive activation of STAT3 in human hepatoma cells

Constitutive phosphorylation of STAT3 at tyrosine 705 was clearly detected in all hepatoma cells, however, STAT3 was only faintly phosphorylated in normal hepatocytes (Fig. 1A). Since JAK2 is one of the major upstream activators of STAT3, we examined the effect of AG490, a JAK2 specific inhibitor, on the STAT3 phosphorylation. AG490 inhibited the phosphorylation of STAT3 in all hepatoma cells, but not in normal hepatocytes. Since SOCS-1 and SOCS-3, negative regulators of the JAK2-STAT3 signaling pathway, are silenced in several hepatoma cells [19,20], we analyzed the expression of SOCS-1 and SOCS-3 by Western blotting. SOCS-1 was detected in Huh-7 and HepG2 but not in Huh-1 or Hep3B, however, SOCS-3 was hardly detected in all hepatoma cells. In contrast, both SOCS-1 and SOCS-3 were detected in normal hepatocytes (Fig. 1B). Next, to determine the extent of constitutive activity of STAT3 in hepatoma cells, the luciferase reporter assay was carried out using a pSTAT3-TA-Luc with or without IL-6 stimulation. The luciferase activity of pSTAT3-TA-Luc without IL-6 stimulation was nearly fourfold higher than that of pTA-Luc which lacks STAT3 binding sequences, and was almost half of that of pSTAT3-TA-Luc with IL-6 stimulation in Huh-1 and Huh-7 (Fig. 1C). Whereas, AG490 dose-dependently repressed the luciferase activity of pSTAT3-TA-Luc in both cells (Fig. 1D). These results indicate that STAT3 is constitutively activated in human hepatoma cells, which is abrogated by AG490.

3.2. AG490 suppresses the growth of human hepatoma cells

We examined the effect of AG490 on the growth of hepatoma cells. AG490 dose-dependently suppressed the growth of all hepatoma cells (Fig. 2A). Next, DNA content in hepatoma cells was analyzed by a flow cytometer (Fig. 2B). In Huh-1, Huh-7 and HepG2, the percentage of both S phase and G2/M phase decreased 24 h after AG490 treatment, and the percentage of G0/G1 phase increased. Whereas, the subG1 population corresponding to the apoptotic cells increased slightly, although more than 48 h incubation with AG490 increased subG1 population more in these cells (data not shown). In contrast, the subG1 population clearly increased 24 h after AG490 treatment in Hep3B (Fig. 2B). These results indicate that the inhibition of constitutive activation of STAT3 induced cell cycle arrest at G0/G1 phase in Huh-1, Huh-7 and HepG2, and induced apoptosis in Hep3B.

To clarify whether the inhibition of STAT3 activity by means of other than AG490 can also repress the growth of hepatoma cells, a cell permeable STAT3 inhibitor peptide was used in the experiments. This phosphopeptide specifically complexes with STAT3 monomers through binding to STAT3-SH2 domain and disrupts the dimerization of STAT3 [13]. Addition of STAT3 inhibitor peptide dose-dependently repressed the luciferase activity of pSTAT3-TA-Luc in Huh-7 and their growth as well as AG490 (Fig. 3).

3.3. AG490 represses the expression of cyclin D1 and anti-apoptotic proteins in human hepatoma cells

Cyclin D1 is a key molecule stimulating G1 to S phase transition and its expression is regulated by STAT3 [2,3]. Western blotting showed that the expression of cyclin D1 was repressed in all hepatoma cells by AG490 (Fig. 4). Whereas, the expression of Waf1/p21 that inhibits G1 to S phase transition was upregulated by AG490 in Huh-7 and Hep3B. In addition, we examined the expression of several anti-apoptotic proteins. Of these, the expression of Bcl-xL and survivin, which are known as STAT3-regulated genes [2,3,5,11] and related with hepatoma development [32,33], was suppressed by AG490 in Huh-1, HepG2 and Hep3B. However, the expression of XIAP was suppressed by AG490 only in Huh-7. The expression of FLIP and CIAP-1, -2 was unchanged by AG490 in all hepatoma cells. In contrast, the expression of Bax, which has an apoptotic-promoting function, was upregulated by AG490 in Hep3B in which AG490 induced apoptosis.

3.4. AG490 sensitizes human hepatoma cells to TRAIL-induced apoptosis

We evaluated whether abrogation of STAT3 signaling by AG490 sensitized human hepatoma cells to TRAIL-induced apoptosis. 2 ng/ml of TRAIL alone slightly induced apoptosis in Huh-1, and did not induce apoptosis in Huh-7 and HepG2 (Fig. 5A). In addition, AG490 alone slightly induced apoptosis in these cells (Fig. 2B). However, the combination of AG490 and

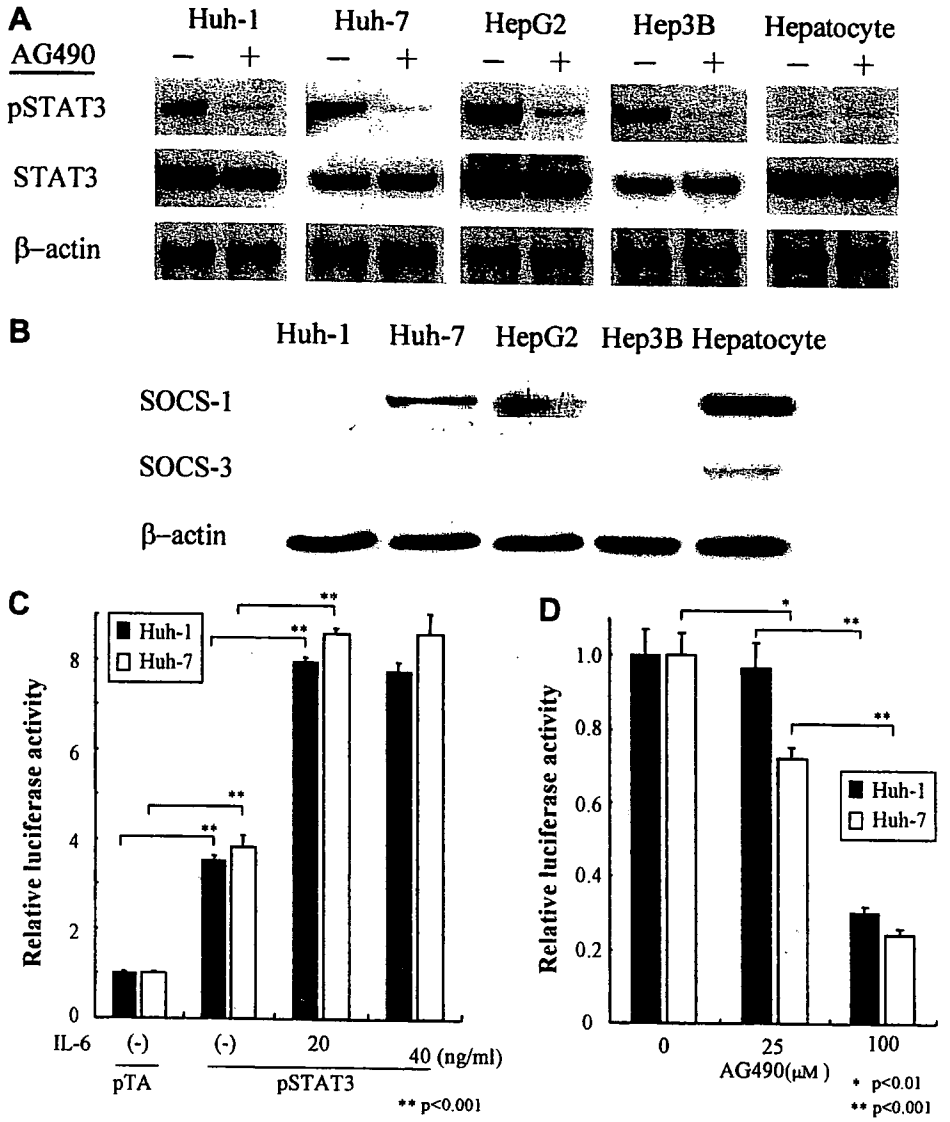

Fig. 1. Effect of AG490 on STAT3 activity in human hepatoma cells (A) Huh-1, Huh-7, HepG2, Hep3B cells and normal human hepatocytes (Hc cells) were incubated with AG490 (+) (100 μM) for 3 h or vehicle (0.1% DMSO) alone as a control (−), after which STAT3 phosphorylation at tyrosine 705 was analyzed by Western blotting. Upper, middle and lower lanes correspond to phosphorylated STAT3, total STAT3 and β-actin, respectively. Results shown are from one representative experiment from a total of four performed. (B) The expression of SOCS-1, SOCS-3 and β-actin in hepatoma cells and normal human hepatocytes (Hc cells) was analyzed by Western blotting. Results shown are from one representative experiment from a total of three performed. (C) pSTAT3-TA-Luc was cotransfected with pRL-CMV-Luc into Huh-1 (closed bar) and Huh-7 (open bar) cells. Six hours later, the cells were incubated with or without IL-6 (20 and 40 ng/ml) for 24 h. Luciferase activity in the cells was analyzed by dual-luciferase assay. Data represent ratios of firefly-Luc activity derived from pSTAT3-TA-Luc over *Renilla*-Luc activity derived from pRL-CMV-Luc relative to the control (pTA-Luc and pRL-CMV-Luc cotransfection without IL-6), and are expressed as mean ± SD of three separate experiments. (D) pSTAT3-TA-luc was cotransfected with pRL-CMV-luc into Huh-1 (closed bar) and Huh-7 (open bar) cells. Six hours later, the cells were incubated with AG490 (25 and 100 μM) for 24 h or vehicle (0.1% DMSO) alone as a control. Luciferase activity in the cells was analyzed by dual-luciferase assay. Data represent ratios of firefly-luc activity derived from pSTAT3-TA-luc over *Renilla*-luc activity derived from pRL-CMV-luc relative to the control, and are expressed as means ± SD of three separate experiments.

TRAIL apparently induced apoptosis in these cells (Fig. 5A).

Next, we determined the effect of AG490 on the expression of TRAIL death receptors, DR4 and DR5. Western blotting showed that DR5 expression was upregulated by AG490 in Huh-1 and Huh-7 but not HepG2, and that DR4 expression was upregulated in HepG2 but unchanged in other cells (Fig. 5B). RT-PCR analysis also showed the AG490-mediated upregulation of DR5 or DR4 mRNA in Huh-7 or HepG2, respectively (Fig. 5C). To know the role of AG490-mediated upregulation of DR5 or DR4, we examined the effects of DR5 and DR4-specific blocking chimera antibodies (DR5-chimera and DR4-chimera) on AG490/TRAIL-induced apoptosis in Huh-7 and HepG2 (Fig. 5D), where DR5-chimera more repressed the AG490/TRAIL-induced apoptosis in Huh-7 than DR4-chimera, in contrast, DR4-chimera more repressed

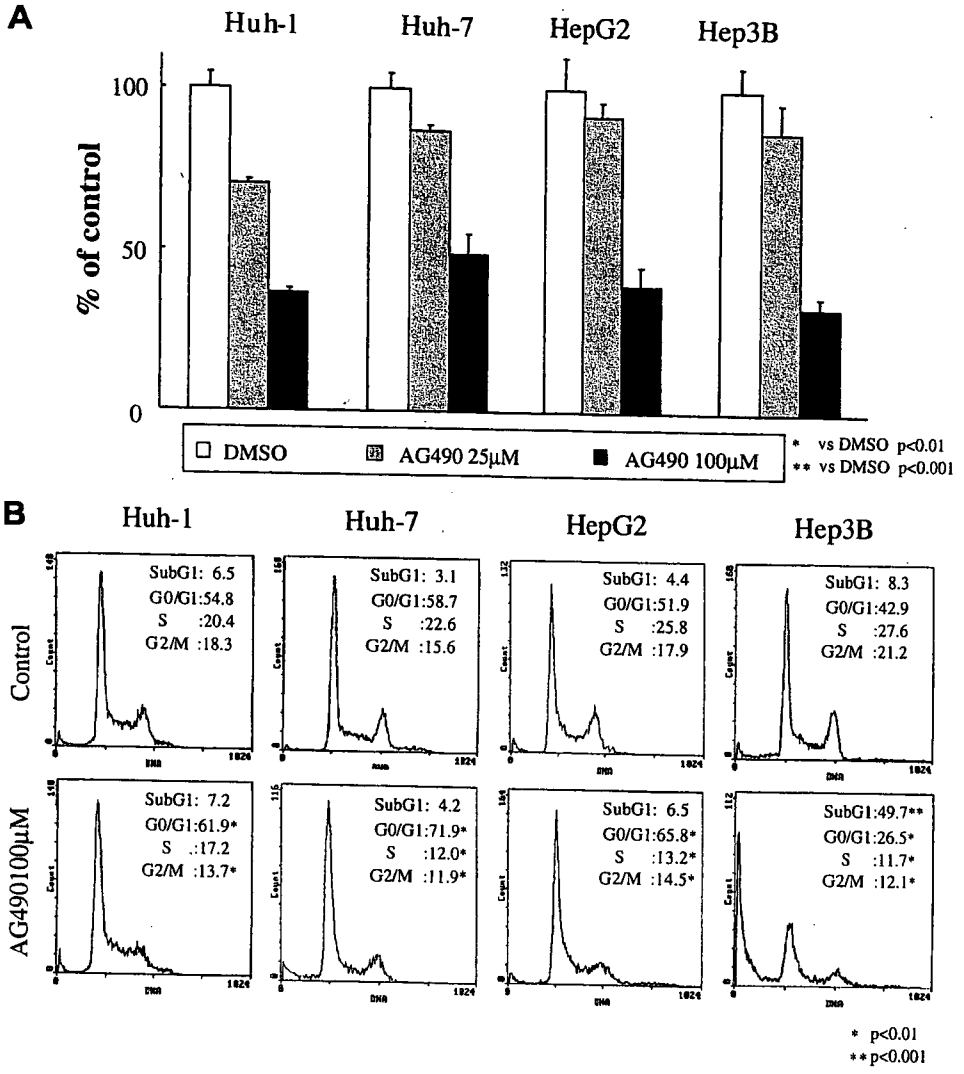

Fig. 2. Effect of AG490 on the cell growth, cell cycle and apoptosis of human hepatoma cells. (A) Huh-1, Huh-7, HepG2 and Hep3B cells were seeded into 24-well plates at a density of 2×10^4 cells per well and incubated with AG490 (25 and 100 μM) for 48 h or vehicle (0.1% DMSO) alone as a control, after which cell number was counted. Results are expressed as a percentage of the control. Data represent means ± SD values of four separate experiments. (B) Huh-1, Huh-7, HepG2 and Hep3B cells were incubated with AG490 (100 μM) for 24 h or vehicle (0.1% DMSO) alone as a control. Cells were then stained with propidium iodide and subjected to DNA content analysis by flow cytometry. Results shown are from one representative experiment from a total of four performed. The mean percentages of cells in G0/G1, S, G2/M and SubG1 from four separate experiments are indicated; $^*p < 0.01$ versus control, $^{**}p < 0.001$ versus control.

those apoptosis in HepG2 than DR5-chimera. These results suggest that AG490-mediated upregulation of DR5 in Huh-7 and DR4 in HepG2, respectively, may contribute to increased susceptibility of these cells to TRAIL.

3.5. Combination of AG490 and TRAIL inhibits the growth of pre-established Huh-7 tumor in an athymic mouse model

Huh-7 cells were subcutaneously inoculated into athymic mice. After the tumor diameter reached more than 5 mm, AG490 (0.5 mg/mouse) and/or TRAIL (40 ng/mouse) was injected into the peritoneal space for 13 days, and tumor growth was monitored (Fig. 6A). AG490-injected mice developed smaller tumor than control ($p < 0.05$) and TRAIL-injected mice ($p < 0.05$). Whereas, injection of both AG490 and TRAIL markedly repressed the growth of tumor compared to control ($p < 0.01$), TRAIL alone ($p < 0.01$) and AG490 alone ($p < 0.01$). The tumor weight at the end of the experiments in the mice treated with both AG490 and TRAIL was also significantly lighter than that in the control mice (406 ± 37 mg versus 2088 ± 285 mg, $P < 0.01$). Histopathological examination with hematoxylin-eosin (HE) staining showed that tumor cell death with condensed nuclei which could be corresponding to apoptotic cells was observed in the tumor tissue from mice treated with both AG490 and TRAIL (Figs. 6B-e and -f). The percentage of cell death

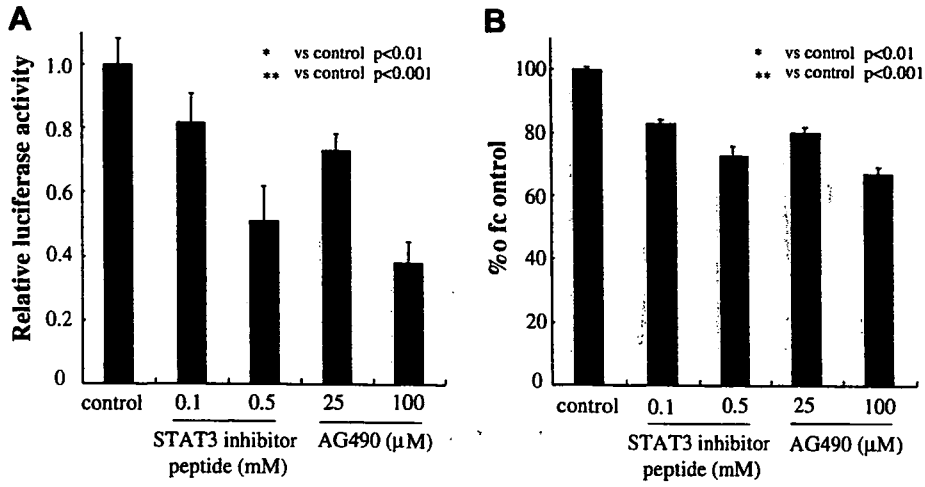

Fig. 3. Effects of STAT3 inhibitor peptide on the STAT3 activity in Huh-7 cells and their growth. (A) pSTAT3-TA-Luc was cotransfected with pRL-CMV-Luc into Huh-7 cells. Six hours later, the cells were cultured alone (control), or with STAT3 inhibitor peptide (0.1 and 0.5 mM) or AG490 (25 and 100 μM) for 24 h. Luciferase activity was determined as described in Fig. 1 legend. Data are expressed as means ± SD values of four separate experiments. (B) Huh-7 cells were cultured alone (control), or with STAT3 inhibitor peptide (0.1 and 0.5 mM) or AG490 (25 and 100 μM) for 24 h, and cell viability was determined by the colorimetric method using a Cell Counting kit (Wako Life Science, Osaka, Japan). Data represent the percentage of control, and are expressed as means ± SD values of four separate experiments.

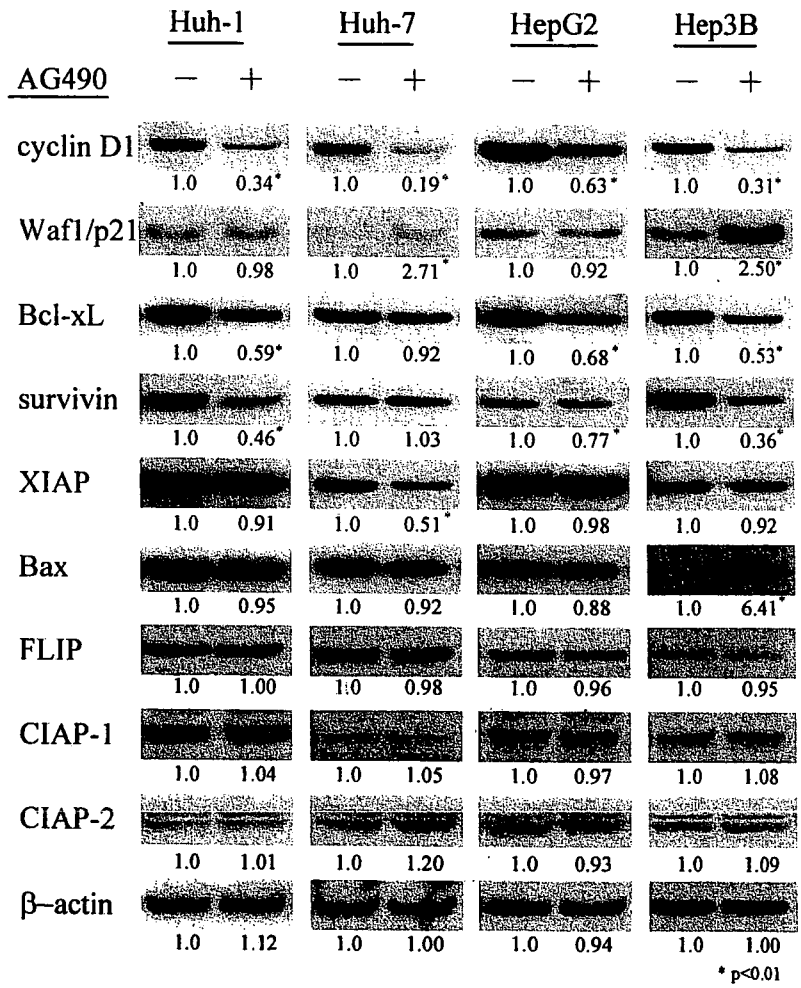

Fig. 4. Effect of AG490 on the expression of cyclin D1, Waf1/p21 and several apoptosis-related proteins in human hepatoma cells. Huh-1, Huh-7, HepG2 and Hep3B cells were incubated with AG490 (+) (100 μM) for 24 h or vehicle (0.1% DMSO) alone as a control (−), and the expression of cyclin D1, Waf1/p21, Bcl-xL, survivin, XIAP, Bax, FLIP, CIAP-1, CIAP-2 and β-actin in the cells was analyzed by Western blotting using the appropriate antibodies. Results shown are from one representative experiment from a total of four performed. The density of each band in the four separate experiments was quantified with NIH image analysis software, and the mean ratio of density relative to control (−) is indicated; *$p < 0.01$ versus control.

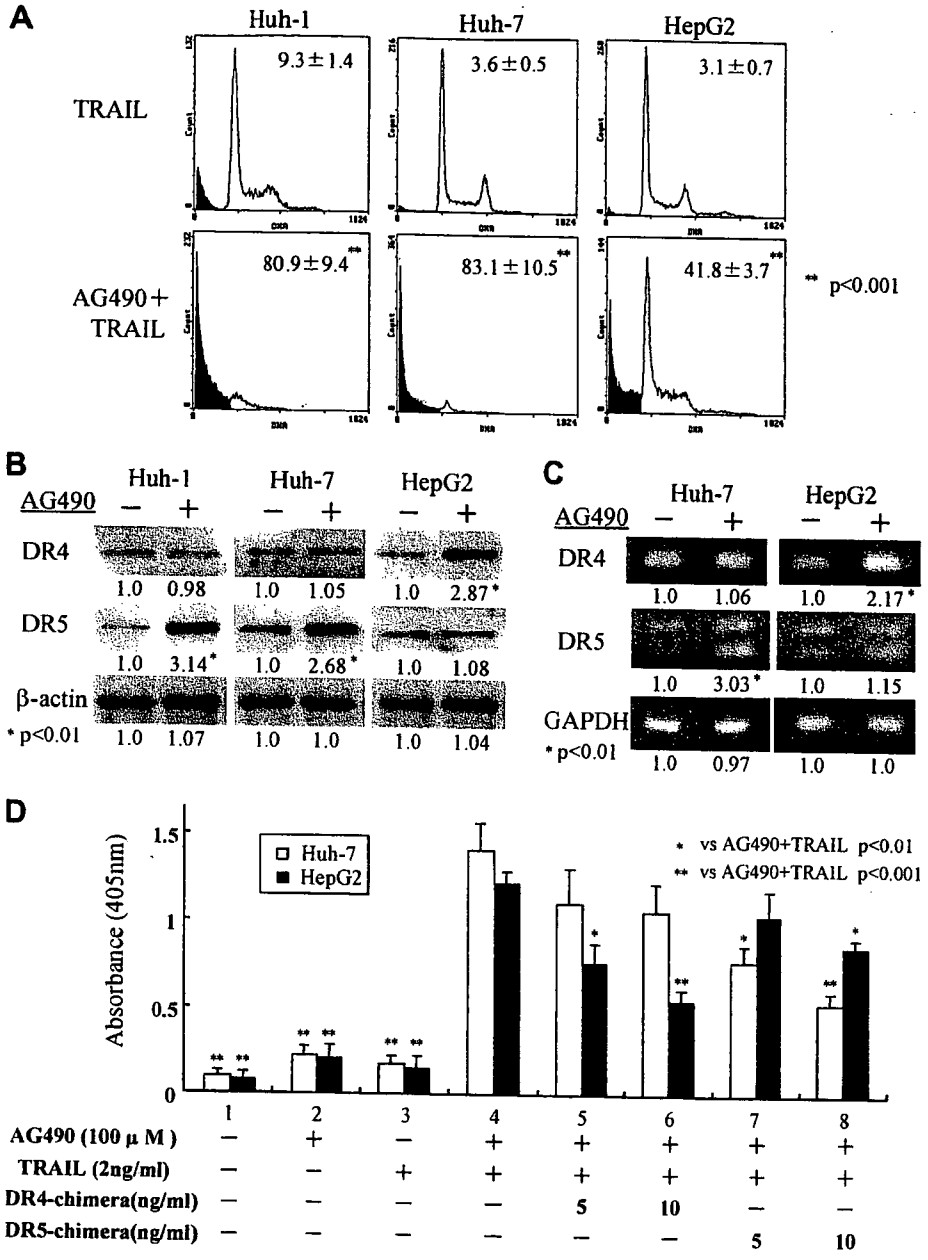

Fig. 5. Effect of AG490 on TRAIL-mediated apoptosis and the expression of DR4 and DR5 in human hepatoma cells. (A) Huh-1, Huh-7 and HepG2 cells were incubated in the presence of TRAIL (2 ng/ml) with or without AG490 (100 μM) for 24 h, and DNA contents were analyzed by flow cytometry. Histograms with black areas represent SubG1 population in the cells. Results shown are from one representative experiment from a total of four performed. Means ± SD percentages of cells in SubG1 from four separate experiments are indicated; $^{**}p < 0.001$ versus control. (B) Huh-1, Huh-7 and HepG2 cells were incubated with AG490(+) (100 μM) for 24 h or vehicle (0.1% DMSO) alone as a control (−) and the expression of DR4, DR5 and β-actin in the cells was analyzed by Western blotting. Results shown are from one representative experiment from a total of five performed. The density of each band in the five separate experiments was quantified with NIH image analysis software, and the mean ratio of density relative to control (−) is indicated; $^{*}p < 0.01$ versus control (−). (C) Huh-7 and HepG2 cells were incubated with AG490(+) (100 μM) for 24 h or vehicle (0.1% DMSO) alone as a control (−) and the m-RNA expression of DR4, DR5 and GAPDH in the cells was analyzed by RT-PCR. The PCR products were electrophoresed on a 1.2% agarose gel and visualized by ethidium bromide staining. Results shown are from one representative experiment from a total of four performed. The density of each band in the four separate experiments was quantified with NIH image analysis software, and the mean ratio of density relative to control (−) is indicated; $^{*}p < 0.01$ versus control (−). (D) Huh-7 (open bar) and HepG2 (closed bar) cells were cultured alone (control; lane 1), or with AG490 (100 μM) (lane 2), TRAIL (2 ng/ml) (lane 3), AG490 + TRAIL (lane 4), AG490 + TRAIL + DR4-chimera; 5 ng/ml (lane 5) or 10 ng/ml (lane 6), AG490 + TRAIL + DR5-chimera; 5 ng/ml (lane 7) or 10 ng/ml (lane 8) for 18 h in 96-well microplates, and apoptotic cells were analyzed by ApoStrand™ ELISA apoptosis detection kit including anti-ssDNA monoclonal antibody and peroxidase-conjugated anti-mouse antibody. Data represent absorbance (405 nm), and are expressed as means ± SD values of four separate experiments.

area measured from HE staining was significantly higher in the tumor tissue from mice treated with AG490 and TRAIL than that from control mice; 58.5 ± 7.4% vs 8.8 ± 3.1%, $p < 0.01$. In contrast, the damage of normal hepatocytes was hardly observed in mice treated with AG490 and TRAIL (Figs. 6B-b and -c) although HE

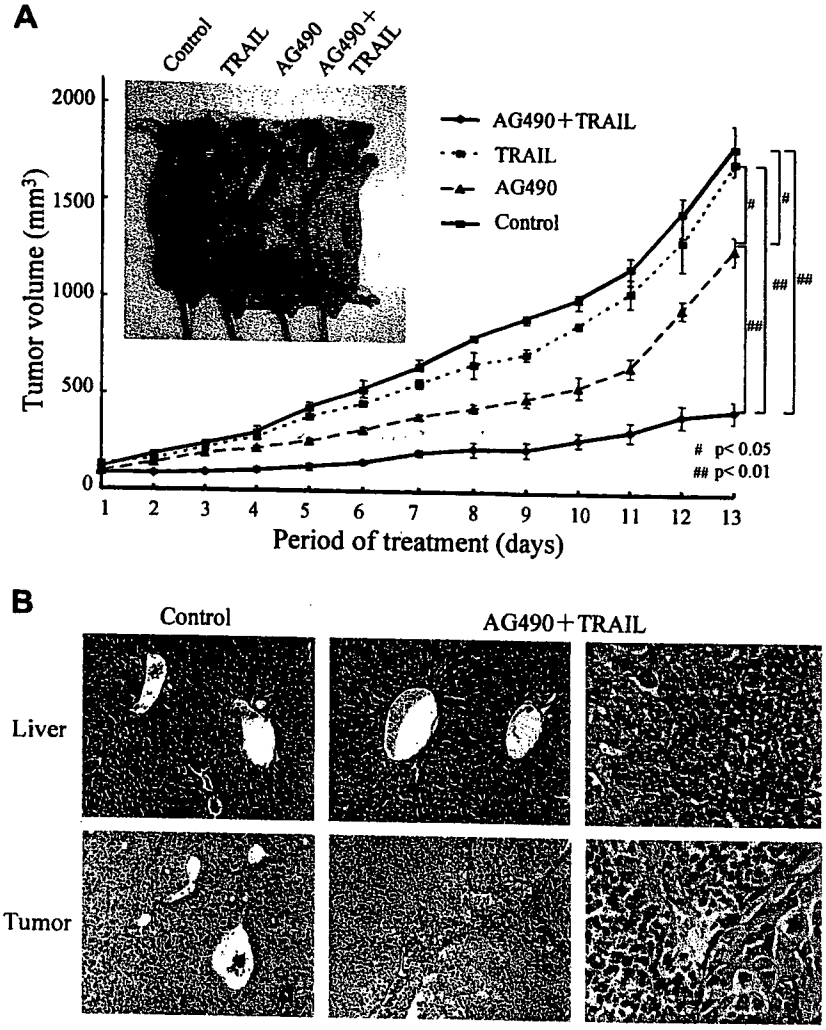

Fig. 6. Anti-tumor effect of combination of AG490 and TRAIL in xenograft models. (A) Huh-7 cells were implanted into athymic mice subcutaneously, and, when tumor diameter reached 5 mm, mice were treated with intraperitoneal injection of vehicle (0.1 ml of 50% DMSO) alone as a control, AG490 (0.5 mg/mouse), TRAIL (40 ng/mouse), and both AG490 (0.5 mg/mouse) and TRAIL (40 ng/mouse) for 13 days, respectively, then tumor growth was monitored as described in Section 2. Data represent means ± SD; *$p < 0.01$ versus control, AG490 alone or TRAIL alone, respectively. Representative photograph of mice after each treatment is also shown. (B) Hematoxylin–eosin (HE) staining of tumors and liver tissues resected from control mouse or mouse treated with both AG490 and TRAIL is shown. a, liver of control mouse; b, liver of mouse treated with both AG490 and TRAIL; c, high magnification of b; d, tumor of control mouse; e, tumor of mouse treated with both AG490 and TRAIL; f, high magnification of e. The percentage of cell death area in each HE-stained tumor specimen was measured with Scion Image (Scion Corporation, Maryland, USA).

staining is not enough to convince the safety of AG490 and TRAIL treatment.

4. Discussion

In the present study, SOCS-1 was silenced in Huh-1 and Hep3B, but not in Huh-7 and HepG2, whereas, SOCS-3 was silenced in all hepatoma cells. In contrast, both SOCS-1 and SOCS-3 were detected in normal human hepatocytes in which the level of STAT3 phosphorylation at tyrosine 705 was much lower than that in hepatoma cells. Taken together, it is possible that both SOCS-1 and SOCS-3 are required for negatively regulating the level of STAT3 phosphorylation in hepatocytes.

Recent studies have shown that src family kinases mediate constitutive STAT3 activation rather than JAK2 in several cancer cells [34–36], and that growth factor receptors such as epidermal growth factor receptor (EGFR) and c-met activate STAT3 through src family kinases [37,38], whereas AG490, a JAK2 specific inhibitor, failed to inhibit the constitutive activation of STAT3 but the src specific inhibitor did. In our study, however, AG490 inhibited the phosphorylation of STAT3 and its transcriptional activity, suggesting that JAK2 is the key kinase involved in the constitutive activation of STAT3 in human hepatoma cells.

Several target genes of STAT3 have been identified including cyclin D1, Bcl-xL, Bcl-2, survivin, mcl-1, c-myc and vascular endothelial growth factor (VEGF) [2–6,12,39] that are essential for cell growth and

survival. These findings are consistent with the reports that abrogation of STAT3 signaling inhibit the growth of various cancer cells and induce apoptosis [9–15]. In the present study, AG490 not only downregulated the expression of cyclin D1 in all hepatoma cells but also upregulated the expression of Waf1/p21 in Huh-7 and Hep3B as reported previously [12], resulting in cell cycle arrest at the G0/G1 phase in Huh-1, Huh-7 and HepG2. On the other hand, AG490 induced apoptosis in Hep3B in which Bax expression was upregulated. In addition, AG490 downregualated the expression of at least one of the anti-apoptotic proteins, Bcl-xL, survivin or XIAP, in all hepatoma cells.

Recent studies have shown that abrogation of STAT3 signaling sensitized cancer cells to chemotherapeutic agents [39,40] and interleukin-12 [41], and that STAT3-inactivated keratinocytes become sensitive to UV-induced apoptosis [42], suggesting that STAT3 signaling pathway protects the cells from various apoptosis stimuli. Therefore, we evaluated whether AG490 sensitized human hepatoma cells to TRAIL-induced apoptosis. TRAIL has been known as a tumor-specific death ligand, however, several cancer cells including hepatoma cells are resistant to TRAIL-induced apoptosis [27]. We have previously reported that interferon (IFN)-α sensitizes human hepatoma cells to TRAIL-induced apoptosis through downregulation of survivin and through upregulation of DR5, a death receptor of TRAIL [43]. In the present study, combination of AG490 and TRAIL apparently induced apoptosis in human hepatoma cells and repressed the growth of Huh-7 tumor in the xenograft model, which could be explained by AG490-mediated downregulation of anti-apoptotic proteins such as Bcl-xL, survivin or XIAP and upregulation of DR4 or DR5 in these cells. Of these, upregulation of DR4 or DR5 by AG490 appears to be essential for increased susceptibility of hepatoma cells to TRAIL because blocking of DR4 or DR5-mediated death signaling by its specific chimera antibody inhibited the synergistic effects of AG490 and TRAIL in inducing apoptosis. However, AG490 did not equally affect the expression of these proteins in hepatoma cells. Furthermore, we only examined the effect of AG490 on the expression of a limited number of cell cycle-related or apoptosis-related proteins. In this regard, Alvarez et al. have recently investigated STAT3 target genes cyclopaedically using microarray analysis and found the rapid induction (within 4.5 h) of several transcription factors including junB, egr1, KLF4, bcl-6 and NFIL3 by STAT3, and proposed that large number of genes are secondarily stimulated by these transcription factors [44]. Surprisingly, they have also revealed that cyclin D1, Bcl-xL and c-myc were not activated by STAT3 at the 4.5 h time point, and speculated that the protein products of other STAT3 target genes are required to collaborate with STAT3 to activate expression of cyclin D1, Bcl-xL and c-myc [44]. Their speculation may also explain the varying effects of AG490 on the expression of apoptosis-related proteins in our study because this expression could be indirectly influenced by AG490 through widespread changes in cellular conditions, which are probably not equivalent in each hepatoma cell.

In conclusion, we have demonstrated in the present study that abrogation of constitutive activation of STAT3 by AG490, JAK2 specific inhibitor, repressed the growth of human hepatoma cells *in vitro*, and greatly enhanced the anti-tumor activity of TRAIL against these cells both *in vitro* and *in vivo* without any adverse effect on normal hepatocytes. These results suggest that the combination of AG490 and TRAIL may have therapeutic potential in the treatment of human HCC.

References

[1] Aaronson DS, Horvath CM. A road map for those who don't know JAK-STAT. Science 2002;296:1653–1655.
[2] Bowman T, Garcia R, Turkson J, Jove R. STATs in oncogenesis. Oncogene 2000;19:2474–2488.
[3] Buettner R, Mora LB, Jove R. Activated STAT signaling in human tumors provides novel molecular targets for therapeutic intervention. Clin Cancer Res 2002;8:945–954.
[4] Wei D, Le X, Zheng L, Wang L, Frey JA, Gao AC, et al. Stat3 activation regulates the expression of vascular endothelial growth factor and human pancreatic cancer angiogenesis and metastasis. Oncogene 2003;22:319–329.
[5] Kanda N, Seno H, Konda Y, Marusawa H, Kanai M, Nakajima T, et al. STAT3 is constitutively activated and supports cell survival in association with survivin expression in gastric cancer cells. Oncogene 2004;23:4921–4929.
[6] Clevenger CV. Roles and regulation of stat family transcription factors in human breast cancer. Am J Pathol 2004;165:1449–1460.
[7] Kusaba T, Nakayama T, Yamazumi K, Yakata Y, Yoshizaki A, Nagayasu T, et al. Expression of p-STAT3 in human colorectal adenocarcinoma and adenoma; correlation with clinicopathological factors. J Clin Pathol 2005;58:833–838.
[8] Hirano T, Ishihara K, Hibi M. Roles of STAT3 in mediating the cell growth, differentiation and survival signals relayed through the IL-6 family of cytokine receptors. Oncogene 2000;19:2548–2556.
[9] Burke WM, Jin X, Lin HJ, Huang M, Liu R, Reynolds RK, et al. Inhibition of constitutively active Stat3 suppresses growth of human ovarian and breast cancer cells. Oncogene 2001;20:7925–7934.
[10] Rahaman SO, Harbor PC, Chernova O, Barnett GH, Vogelbaum MA, Haque SJ. Inhibition of constitutively active Stat3 suppresses proliferation and induces apoptosis in glioblastoma multiforme cells. Oncogene 2002;21:8404–8413.
[11] Aoki Y, Feldman GM, Tosato G. Inhibition of STAT3 signaling induces apoptosis and decreases survivin expression in primary effusion lymphoma. Blood 2003;101:1535–1542.
[12] Scholz A, Heinze S, Detjen KM, Peters M, Welzel M, Hauff P, et al. Activated signal transducer and activator of transcription 3 (STAT3) supports the malignant phenotype of human pancreatic cancer. Gastroenterology 2003;125:891–905.
[13] Turkson J, Ryan D, Kim JS, Zhang Y, Chen Z, Haura E, et al. Phosphotyrosyl peptides block Stat3-mediated DNA binding

activity, gene regulation, and cell transformation. J Biol Chem 2001;276:45443–45455.
[14] Leong PL, Andrews GA, Johnson DE, Dyer KF, Xi S, Mai JC, et al. Targeted inhibition of Stat3 with a decoy oligonucleotide abrogates head and neck cancer cell growth. Proc Natl Acad Sci USA 2003;100:4138–4143.
[15] Mora LB, Buettner R, Seigne J, Diaz J, Ahmad N, Garcia R, et al. Constitutive activation of Stat3 in human prostate tumors and cell lines: direct inhibition of Stat3 signaling induces apoptosis of prostate cancer cells. Cancer Res 2002;62:6659–6666.
[16] Chan KS, Sano S, Kiguchi K, Anders J, Komazawa N, Takeda J, et al. Disruption of Stat3 reveals a critical role in both the initiation and the promotion stages of epithelial carcinogenesis. J Clin Invest 2004;114:720–728.
[17] Tiollais P, Pourcel C, Dejean A. The hepatitis B virus. Nature 1985;317:489–495.
[18] Kiyosawa K, Sodeyama T, Tanaka E, Gibo Y, Yoshizawa K, Nakano Y, et al. Interrelationship of blood transfusion, non-A, non-B hepatitis and hepatocellular carcinoma: analysis by detection of antibody to hepatitis C virus. Hepatology 1990;12:671–675.
[19] Yoshikawa H, Matsubara K, Qian GS, Jackson P, Groopman JD, Manning JE, et al. SOCS-1, a negative regulator of the JAK/STAT pathway, is silenced by methylation in human hepatocellular carcinoma and shows growth-suppression activity. Nat Genet 2001;28:29–35.
[20] Niwa Y, Kanda H, Shikauchi Y, Saiura A, Matsubara K, Kitagawa T, et al. Methylation silencing of SOCS-3 promotes cell growth and migration by enhancing JAK/STAT and FAK signalings in human hepatocellular carcinoma. Oncogene 2005;24:6406–6417.
[21] Feng DY, Zheng H, Tan Y, Cheng RX. Effect of phosphorylation of MAPK and Stat3 and expression of c-fos and c-jun proteins on hepatocarcinogenesis and their clinical significance. World J Gastroenterol 2001;7:33–36.
[22] Liu P, Kimmoun E, Legrand A, Sauvanet A, Degott C, Lardeux B, et al. Activation of NF-kappa B, AP-1 and STAT transcription factors is a frequent and early event in human hepatocellular carcinomas. J Hepatol 2002;37:63–71.
[23] Waris G, Turkson J, Hassanein T, Siddiqui A. Hepatitis C virus (HCV) constitutively activates STAT-3 via oxidative stress: role of STAT-3 in HCV replication. J Virol 2005;79:1569–1580.
[24] Yoshida T, Hanada T, Tokuhisa T, Kosai K, Sata M, Kohara M, et al. Activation of STAT3 by the hepatitis C virus core protein leads to cellular transformation. J Exp Med 2002;196:641–653.
[25] Walczak H, Miller RE, Ariail K, Gliniak B, Griffith TS, Kubin M, et al. Tumoricidal activity of tumor necrosis factor-related apoptosis-inducing ligand in vivo. Nat Med 1999;5:157–163.
[26] Ashkenazi A, Pai RC, Fong S, Leung S, Lawrence DA, Marsters SA, et al. Safety and antitumor activity of recombinant soluble Apo2 ligand. J Clin Invest 1999;104:155–162.
[27] Yamanaka T, Shiraki K, Sugimoto K, Ito T, Fujikawa K, Ito M, et al. Chemotherapeutic agents augment TRAIL-induced apoptosis in human hepatocellular carcinoma cell lines. Hepatology 2000;32:482–490.
[28] Lacour S, Hammann A, Wotawa A, Corcos L, Solary E, Dimanche-Boitrel MT. Anticancer agents sensitize tumor cells to tumor necrosis factor-related apoptosis-inducing ligand-mediated caspase-8 activation and apoptosis. Cancer Res 2001;61:1645–1651.
[29] Chinnaiyan AM, Prasad U, Shankar S, Hamstra DA, Shanaiah M, Chenevert TL, et al. Combined effect of tumor necrosis factor-related apoptosis-inducing ligand and ionizing radiation in breast cancer therapy. Proc Natl Acad Sci USA 2000;97:1754–1759.
[30] Nakabayashi H, Taketa K, Yamane T, Miyazaki M, Miyano K, Sato J. Phenotypical stability of a human hepatoma cell line, HuH-7, in long-term culture with chemically defined medium. Gann 1984;75:151–158.
[31] Osawa Y, Banno Y, Nagaki M, Brenner DA, Naiki T, Nozawa Y, et al. TNF-alpha-induced sphingosine 1-phosphate inhibits apoptosis through a phosphatidylinositol 3-kinase/Akt pathway in human hepatocytes. J Immunol 2001;167:173–180.
[32] Takehara T, Liu X, Fujimoto J, Friedman SL, Takahashi H. Expression and role of Bcl-xL in human hepatocellular carcinomas. Hepatology 2001;34:55–61.
[33] Notarbartolo M, Cervello M, Giannitrapani L, Meli M, Poma P, Dusonchet L, et al. Expression of IAPs and alternative splice variants in hepatocellular carcinoma tissues and cells. Ann N Y Acad Sci 2004;1028:289–293.
[34] Niu G, Bowman T, Huang M, Shivers S, Reintgen D, Daud A, et al. Roles of activated Src and Stat3 signaling in melanoma tumor cell growth. Oncogene 2002;21:7001–7010.
[35] Xi S, Zhang Q, Dyer KF, Lerner EC, Smithgall TE, Gooding WE, et al. Src kinases mediate STAT growth pathways in squamous cell carcinoma of the head and neck. J Biol Chem 2003;278:31574–31583.
[36] Laird AD, Li G, Moss KG, Blake RA, Broome MA, Cherrington JM, et al. Src family kinase activity is required for signal transducer and activator of transcription 3 and focal adhesion kinase phosphorylation and vascular endothelial growth factor signaling in vivo and for anchorage-dependent and -independent growth of human tumor cells. Mol Cancer Ther 2003;2:461–469.
[37] Song L, Turkson J, Karras JG, Jove R, Haura EB. Activation of Stat3 by receptor tyrosine kinases and cytokines regulates survival in human non-small cell carcinoma cells. Oncogene 2003;22:4150–4165.
[38] Silva CM. Role of STATs as downstream signal transducers in Src family kinase-mediated tumorigenesis. Oncogene 2004;23:8017–8023.
[39] Real PJ, Sierra A, De Juan A, Segovia JC, Lopez-Vega JM, Fernandez-Luna JL. Resistance to chemotherapy via Stat3-dependent overexpression of Bcl-2 in metastatic breast cancer cells. Oncogene 2002;21:7611–7618.
[40] Alas S, Bonavida B. Inhibition of constitutive STAT3 activity sensitizes resistant non-Hodgkin's lymphoma and multiple myeloma to chemotherapeutic drug-mediated apoptosis. Clin Cancer Res 2003;9:316–326.
[41] Burdelya L, Catlett-Falcone R, Levitzki A, Cheng F, Mora LB, Sotomayor E, et al. Combination therapy with AG-490 and interleukin 12 achieves greater antitumor effects than either agent alone. Mol Cancer Ther 2002;1:893–899.
[42] Sano S, Chan KS, Kira M, Kataoka K, Takagi S, Tarutani M, et al. Signal transducer and activator of transcription 3 is a key regulator of keratinocyte survival and proliferation following UV irradiation. Cancer Res 2005;65:5720–5729.
[43] Shigeno M, Nakao K, Ichikawa T, Suzuki K, Kawakami A, Abiru S, et al. Interferon-alpha sensitizes human hepatoma cells to TRAIL-induced apoptosis through DR5 upregulation and NF-kappa B inactivation. Oncogene 2003;22:1653–1662.
[44] Alvarez JV, Febbo PG, Ramaswamy S, Loda M, Richardson A, Frank DA. Identification of a genetic signature of activated signal transducer and activator of transcription 3 in human tumors. Cancer Res 2005;65:5054–5062.

Hep Intl (2007) 1:287–294
DOI 10.1007/s12072-007-9007-4

ORIGINAL PAPER

Role of growth hormone, insulin-like growth factor 1 and insulin-like growth factor-binding protein 3 in development of non-alcoholic fatty liver disease

Tatsuki Ichikawa · Kazuhiko Nakao · Keisuke Hamasaki · Ryuji Furukawa · Shotarou Tsuruta · Yasuo Ueda · Naota Taura · Hidetaka Shibata · Masumi Fujimoto · Kan Toriyama · Katsumi Eguchi

Received: 14 April 2007 / Published online: 1 June 2007

Abstract
Background and aims Pituitary dysfunction including growth hormone (GH) deficiency may be associated with non-alcoholic fatty liver disease (NAFLD). Since the relationships among GH, IGF-1, IGFBP-3, and development of NAFLD without hypopituitarism are unclear, we examined the role of these hormones in the development of NAFLD based on clinical, laboratory and liver histology data.
Patients and methods A total of 55 consecutive patients (20 males and 35 females) with NAFLD.
Results Aspartate amino transferase (AST), AST/ALT, platelet count and IGF-1, levels were significantly associated with differences in fibrosis, since these variables differed between stage 0–1 and stage 2–3 NAFLD. In multivariate analysis, platelet count ($P = 0.0223$, relative risk (RR), 5.899; 95% confidence interval (CI), 1.288–27.017), and IGF-1 ($P = 0.0363$, RR, 4.568; 95% CI, 1.101–18.945) showed significant associations with stage 2–3 NAFLD. Additionally, hyaluronic acid levels had a negative relationship with IGF-1 and the IGF-1/IGFBP-3 ratio. There was no relationship of fibrosis with GH level, but decreased GH ($P = 0.0414$, RR, 0.199; 95% CI, 0.042–0.989) was significantly associated with steatosis of stage 2–3. Low GH/IGF-1 and GH/IGFBP-3 ratios were found in advanced steatosis.
Conclusion GH, IGF-1 and IGFBP-3 are associated with hepatic fibrosis and steatosis in NAFLD. Low levels of IGF-1 might be associated with fibrosis while low level of GH with hepatic steatosis.

Keywords Non-alcoholic fatty liver disease · Growth hormone · Insulin-like growth factor 1 · Insulin-like growth factor-binding protein 3 · Stage

Abbreviations

ALP	Alkaline phosphatase
ALT	Alanine aminotransferase
AST	Aspartate aminotransferase
γ-GTP	γ-Glutamyltranspeptidase
BMI	Body mass index
CT	Computed tomography
FMV	Flow-mediated vasodilatation
GH	Growth hormone
IGF-1	Insulin-like growth factor 1
IGFBP-3	Insulin-like growth factor-binding protein 3
IMT	Intima-media thickness
NAFLD	Non-alcoholic fatty liver disease
NASH	Non-alcoholic steatohepatitis
STAT	Signal transducers and activators of transcription
US	Ultrasonography

Introduction

Striking similarities exist between the metabolic syndrome and untreated GH deficiency (GHD) in adults, and

T. Ichikawa (✉) · K. Nakao · K. Hamasaki · N. Taura · H. Shibata · M. Fujimoto · K. Eguchi
The First department of Internal Medicine, Graduate school of Biomedical science, Nagasaki University, 1-7-1 Sakamoto, Nagasaki 852-8501, Japan
e-mail: ichikawa@net.nagasaki-u.ac.jp

R. Furukawa · S. Tsuruta · Y. Ueda
Department of Internal Medicine, The Japanese Red Cross Nagasaki Atomic Bomb Hospital, Nagasaki, Japan

K. Toriyama
Department of Pathology, Institute of Tropical medicine, Nagasaki University, Nagasaki, Japan

undetectable and low levels of GH may be of importance in the metabolic aberrations observed in both conditions [1]. Together with atherosclerosis, visceral obesity, hypertension, hyperlipidemia, and insulin resistance. Non-alcoholic fatty liver disease (NAFLD) is a common feature in metabolic syndrome and in hypopituitaric and hypothalamic dysfunction [2, 3]. Lonardo et al. showed that low levels of GH are independent predictors of NAFLD in male patients [4], and recent reports suggest that hypothalamic and/or pituitary disease including GHD involves a rapid progressive NAFLD [3]; the reason for rapid progression was speculated to be body weight gain, and not GHD itself. We have previously found an association of adult onset GHD with NAFLD [2], and shown that hepatic steatosis is more frequently observed in patients with GHD than in those without GHD, suggesting that adult onset GHD is a possible risk factor for NAFLD. However, the role of GH in NAFLD remains unclear, despite the growing knowledge of the activity of this hormone in induction of lipolysis and lipid oxidation [5].

IGF-1 is secreted from hepatocytes by GH stimulation. It is a catabolic hormone with a role in protein synthesis, and can also stimulate secretion of IGFBP-3 from Kupffer cells [6]. The biological activity of IGF-1 is strongly influenced by several IGF-specific binding proteins (IGFBP-1 to 6), of which IGFBP-3 carries >80% of circulating IGF-1 [7]. The presence of IGFBP-3 lowers IGF-1 bioactivity [8], and the ratio between IGF-1 and IGFBP-3 levels decreases with increasing age in adults, resulting in decreased levels of free and biologically active IGF-1 [9]. IGF-1 has been shown to have a protective effect on ischemic heart disease, cardiovascular disease mortality and atherosclerosis [7, 10, 11], whereas high levels of IGFBP-3 and a low IGF-1/IGFBP-3 ratio are correlated with atherosclerosis [9]. Cardiovascular disease is a serious problem in NAFLD patients, and ischemic heart disease is a major cause of death among these patients [12]. NAFLD is associated with advanced carotid atherosclerosis [13] and endothelial dysfunction, and the 10-year probability of occurrence of cardiovascular events [14], and especially intima-media thickness (IMT) has a strong association with the degree of hepatic fibrosis in NAFLD patients [15].

Although GH levels have been correlated with metabolic syndrome, and IGF-1 and IGFBP-3 are related to cardiovascular disease, the relationships among GH, IGF-1, IGFBP-3, and the severity of NAFLD have not been examined. Therefore, the aim of this study was to compare GH, IGF-1, and IGFBP-3 levels with the degree of fibrosis, inflammation and steatosis in NAFLD patients, and to clarify the relationship between the development of NAFLD and the levels of these hormones.

Patients and methods

Patients

The study included 55 consecutive patients (20 males and 35 females) with NAFLD who attended the First Department of Internal Medicine at the Graduate School of Biomedical Science, Nagasaki University and the Department of Internal Medicine at the Japanese Red Cross Nagasaki Atomic Bomb Hospital, with an initial visit between April 1998 and December 2005. NAFLD was diagnosed on the basis of a persistently raised ALT level (>1.5 times the upper normal limit for 6 months or more) and on US and CT images. A percutaneous liver biopsy assisted by US was performed in all cases, and scored using the criteria proposed by Brunt et al. [16]. Liver biopsy specimens were fixed in 10% formalin, embedded in paraffin, cut to a thickness of 4 μm, and subjected to hematoxylin-eosin, and Azan-Mallory staining. All liver tissue specimens were evaluated by a single pathologist who was blinded to the clinical condition of the patient. Patients with positive hepatitis B and C serology or with evidence of inherited, autoimmune, cholestatic, or drug-induced liver disease were excluded using standard clinical, laboratory, imaging, and histological criteria. In addition, the subjects included in the study had no history of current or past excessive alcohol intake, as defined by an average daily consumption of more than 20 g of alcohol. At the time of the study, none of the patients showed clinical, biochemical or histological evidence of cirrhosis. Of the 55 cases that were originally included in the study, three secondary cases of NAFLD were subsequently excluded: two of these cases were steatohepatitis after pancreatoduodenal resection, and the third was a case of adult onset hypopituitarism.

Clinical and laboratory measurements

Body mass index (BMI) was calculated as weight (kg) divided by the square of height (m). Subjects fasted overnight before blood samples were obtained. Venous plasma glucose was measured with an automated analyzer, and basal serum insulin was measured using a standard radioimmunoassay. The index of insulin resistance was calculated using the fasting value of plasma glucose, (we excluded the patients with greater than 130 mg/dl), and the serum insulin level, according to the homeostasis model assessment (HOMA) method. Hemoglobin A1c, ALT, AST, γ-GTP, ALP, total cholesterol, triglyceride, C-reactive protein and ferritin, and hyaluronic acid were determined by standard hematometry and laboratory techniques. Measurements of GH, IGF-1. and IGFBP-3 were performed using commercially available kits. The sensitivity

of the serum GH, IGF-1, and IGFBP-3 assay was 0.02 ng/ml, 4 μg/l, and 0.20 mg/l, respectively. The GH/IGF-1, GH/IGFBP-3, and IGF-1/IGFBP-3 concentration ratios were estimated to get a better understanding of the relative changes in concentration of GH, IGF-1, and IGFBP-3.

Statistical analysis

Data were processed on a personal computer and analyzed using StatView 5.0 (SAS Institute, Inc., Cary, NC). Differences between groups were analyzed by Mann–Whitney test and Pearson χ^2 test. Correlation analysis was carried out using Spearmen rank correlation. Logistic regression analysis was used to test the association of variables with different stages of NAFLD and steatosis. All data in the text and tables are given as means, unless otherwise indicated. Variables that achieved statistical significance in the univariate analysis were subsequently included in a multivariate analysis using a logistic regression model, and described as odds ratios (OR) with 95% CI. Spearman rank correlation was used to examine the relationship between variables. Values of $P < 0.05$ were considered statistically significant.

Results

Subject characteristics

Clinical and laboratory data for the 52 NAFLD subjects are shown in Table 1. BMI (kg/m^2) was distributed as follows: BMI<25 in eight cases; BMI 25–30 in 27 cases; BMI 30–35 in 13 cases, BMI 35–40 in three cases, and BMI >40 in one case. The HOMA-IR score reflects insulin resistance, with a score of >2.5 indicating insulin resistance in Japanese subjects [17]. The mean HOMA-IR index in our subjects was 4.05, and 26 cases (70%) had values in excess of 2.5. The normal range of serum GH concentration is <0.17 ng/ml in males and 0.28–1.64 ng/ml in females. Of the 35 females with NAFLD in the study, 24 (73%) had GH levels less than the normal range, while in the others this was within the normal limits. In contrast, 11 of the 20 male NAFLD patients (58%) had GH levels above the normal range for males, and the remaining eight cases (42%) were within the normal limits. For IGF-1, the normal ranges in males aged 17–20, 21–30, 31–40, 41–50, 51–60, 61–70 and >70-years-old are 219–509, 85–369, 67–318, 41–272, 59–215, 42–250, 75–218 μg/l, respectively, whereas in females these data are 264–542, 119–389, 73–311, 46–282, 37–266, 37–150, 38–207 μg/l, respectively. In this study, three patients (one male and two female) had IGF-1 levels below the normal range for their age, and two patients (both females) had IGF-1 levels higher than the normal range. Regarding IGFBP-3, the normal ranges in people aged 17–35 and 36–70 years old were 2.29–4.17 and 2.17–4.05 mg/l, respectively, and 12 female patients (35%) and seven male patients (37%) had IGFBP-3 levels less than the normal limit for their age. Hence, aberrant values of serum IGF-1 concentration were found in a few cases, IGFBP-3 levels lower than the normal range were found in more than 30% of NAFLD patients.

Clinical and laboratory data in NAFLD patients at stages 0–1 and 2–3

The NAFLD patients who were classified into stages and clinical and laboratory data were compared between stage 0–1 and stage 2–3 patients (Table 1). There were no differences in sex, age, BMI, ALT, γ-GTP, ALP, total cholesterol, triglyceride, C-reactive protein, white blood cell count, red blood cell count, GH, IGFBP-3, insulin, HOMA-IR score, and HbA1c between the two groups. However, AST ($P = 0.0005$) and AST/ALT ($P = 0.0206$) were lower in stage 0–1 patients, and platelet count ($P = 0.002$) and IGF-1 ($P = 0.0272$) were higher in stage 0–1 patients, compared to stage 2–3 patients.

Univariate and multivariate analysis of risk factors for stage 2–3 NAFLD

The results of univariate and multivariate analyses of risk factors for stage 2–3 NAFLD are shown in Table 2. In the univariate analysis, the following three factors were significantly associated with stage 2–3 NAFLD: reduced AST (relative risk (RR), 0.238; 95% confidence interval (CI), 0.069–0.824 [$P = 0.0235$]), reduced platelet count (RR, 4.667; 95% CI, 1.301–16.739 [$P = 0.0181$]), and reduced IGF-1 level (RR, 4.643; 95% CI, 1.331–16.196 [$P = 0.016$]). In a multivariable analysis, reduced platelet count (RR, 5.899; 95% CI, 1.288–27.017 [$P = 0.0223$]) and reduced IGF-1 (RR, 4.568; 95% CI, 1.101–18.945 [$P = 0.0363$]) were significantly associated with stage 2–3 NAFLD.

Correlation between serum hyaluronic acid and the GH/IGF-1/IGFBP-3 axis

Hyaluronic acid is a hepatic fibrosis marker [18], and its correlation with GH, IGF-1 and IGFBP-3 was explored in 41 NAFLD patients in whom the level was within the detection range of the assay (Table 3). The GH level showed no correlation with hyaluronic acid, but IGF-1 and IGFBP-3 levels showed a negative correlation with the hyaluronic acid level, with the IGF-1 level showing a

Table 1 Clinical and laboratory data for NAFLD patients at stages 0–1 and 2–3

Item	Total (n = 52)	Stage 0–1 (n = 34)	Stage 2–3 (n = 18)	P-value
Sex (M/F)	19/33	13/21	6/12	NS
Age (year)	49.7 (17.1)	47.5 (16.7)	55.4 (17.5)	NS
BMI (kg/m^2)	29.0 (4.12)	29.2 (4.4)	28.7 (3.6)	NS
ALT (IU/l)	93.5 (79.1)	76.3 (53.0)	126.0 (107.8)	NS
AST (IU/l)	62.0 (49.8)	45.3 (25.2)	93.7 (67.8)	0.0005
AST/ALT	0.714 (0.226)	0.67 (0.20)	0.80 (0.26)	0.0206
γ-GTP (IU/l)	85.7 (87.2)	67.4 (46.2)	120.3 (129)	NS
ALP (IU/l)	239.0 (71.7)	234.8 (69.3)	246.8 (77.6)	NS
Total cholesterol (mg/dl)	203.1 (35.5)	209.4 (37.6)	191.5 (28.7)	NS
Triglyceride (mg/dl)	161.2 (65.8)	161.1 (64.1)	161.5 (70.7)	NS
C-reactive protein (mg/dl)	0.26 (0.25)	0.251 (0.292)	0.271 (0.187)	NS
White blood cells (μl)	6482 (1664)	6641 (1628)	6683 (1737)	NS
Red blood cells (10^4/μl)	465 (54.6)	473 (45.7)	452 (67.6)	NS
Ferritin (mg/dl)	322 (412.2)	247 (162)	415 (619)	NS
Platelets (μl)	23300 (6300)	24800 (6378)	20400 (5119)	0.002
GH (ng/ml)	0.31 (0.36)	0.298 (0.374)	0.331 (0.357)	NS
IGF-1 (μg/l)	171 (111.8)	191.8 (128)	129.2 (45.4)	0.0272
IGFBP-3 (mg/l)	2.45 (0.66)	2.56 (0,73)	2.24 (0.42)	NS
Insulin (IU/l)	14.8 (6.88)	13.9 (5.56)	16.4 (9.03)	NS
Fasting plasma glucose (mg/l)	113.0 (33.3)	109.4 (30.4)	119.8 (38.4)	NS
HOMA-IR	4.03 (2.4)	3.86 (2.18)	4.40 (2.88)	NS
HbA1c (%)	6.70 (1.9)	6.77 (2.09)	6.48 (1.63)	NS

Data are shown as means (standard deviation) and numbers, with statistical analysis using a Mann–Whitney test for means and a Pearson χ^2 test for numbers

Normal values in laboratory tests: ALT (IU/l), 5–40; AST (IU/l), 10–40; γ-GTP (IU/l), <70 in males, <30 in females; ALP (IU/l), 115–359; total cholesterol (mg/dl), 150–219; triglyceride (mg/dl), 50–149; C-reactive protein (mg/dl), <0.30; white blood cell count (μl), 3900–9800 in males, 3500–9100 in females; red blood cell count (10^4/μl), 427–570 in males, 376–500 in females; ferritin (mg/dl), 27–320 in males, 3.4–89 in females; platelet (μl), 13.1–36.2 in males, 13–36.9 in females; insulin (IU/l), 3.06–16.9; fasting plasma glucose (mg/l), 70–109; HbA1c (%), 4.3–5.8. BMI, GH, IGF-1, IGFBP-3 and HOMA-IR are described in the text

Table 2 Variables independently associated with NAFLD of stages 2–3

Variable	Univariate analysis		Multivariate analysis	
	P-value	RR (95% CI)	P-value	RR (95% CI)
AST	0.0235	0.238 (0.069–0.824)	0.0834	0.282 (0.067–1.182)
Platelet count	0.0181	4.667 (1.301–16.739)	0.0223	5.899 (1.288–27.017)
IGF-1	0.016	4.643 (1.331–16.196)	0.0363	4.568 (1.101–18.945)

The reference groups are AST ≤ 50 IU/l, platelet count < 200,000/l, and IGF-1 < 140 μg/l

Table 3 Correlation between serum hyaluronic acid and the GH/IGF-1/IGFBP-3 axis (n = 41)

Variable	Correlation coefficient	P-value
GH	0.135	NS
IGF-1	–0.427	0.0043
IGFBP-3	–0.352	0.0216
GH/IGF-1	0.338	0.0282
GH/IGFBP-3	0.175	NS
IGF-1/IGFBP-3	–0.436	0.0035

particularly strong negative correlation. As a reflection of these results, the GH/IGF-1 ratio, but not the GH/IGFBP-3 ratio, showed a positive correlation with the hyaluronic acid level, and similarly the IGF-1/IGFBP-3 ratio was positively correlated with hyaluronic acid.

Histopathology and the IGF-1 axis

Due to the negative correlation between IGF-1 and fibrosis, the relationships of IGF-1 with some aspects of

Brunt's fibrosis classification were evaluated. Patients were categorized based on the presence and absence of pericellular fibrosis, portal fibrosis, bridging fibrosis, and ballooning. No differences in IGF-1 were found for groups with and without pericellular fibrosis and bridging fibrosis, but IGF-1 was significantly lower in patients with portal fibrosis (stages 1–3) than in those without portal fibrosis ($P = 0.0229$), and the IGF-1/IGFBP-3 ratio showed a tendency to decrease in patients with portal fibrosis ($P = 0.0837$). In addition, the IGF-1 level was relatively low in patients showing ballooning ($P = 0.0816$) (Fig. 1). The relationship between histological grade of stages 0–1 or 2–3 was also examined, but no correlation was found.

Clinical and laboratory data in patients with steatosis of grade 1 and grades 2–3

The role of the GH/IGF-1/IGFBP-3 axis in steatosis was investigated by grouping patients into grades 1 and grades 2–3 using Brunt's steatosis classification (Table 4). There were no differences in sex, age, BMI, AST, ALT, γ-GTP, ALP, triglyceride, C-reactive protein, white blood cell count, red blood cell count, IGFBP-3, insulin, HOMA-IR score, and HbA1c between the two groups. However, total cholesterol ($P = 0.034$) and IGF-1 level ($P = 0.0180$) were higher in steatosis 2–3 patients and the GH level ($P = 0.0236$) was higher in steatosis 1 patients. In the multivariate analysis, a reduced GH level showed a significant association with steatosis of grades 2–3: GH (RR, 0.43; 95% CI, 0.002–0.772 [$P = 0.0328$]).

The results of univariate and multivariate analyses of risk factors for steatosis of grade 2–3 are shown in Table 5. In the univariate analysis, the following three factors were significantly associated with steatosis of grade 2–3: GH (RR, 0.196; 95% CI 0.046–0.830 [$P = 0.0269$]) and IGF (RR, 4.00; 95% CI, 1.151–13.901 [$P = 0.0291$]). In a multivariable analysis, GH (RR, 0.199; 95% CI, 0.042–0.989 [$P = 0.0414$]) was significantly associated with steatosis of grade 2–3.

Hepatic steatosis score and the GH axis

Correlations of hepatic steatosis score with GH, IGF-1, and IGFBP-3 levels were explored by examining differences in the GH/IGF-1, GH/IGFBP-3, and IGF-1/IGFBP-3 ratios between patients with steatosis of grade 1 and grades 2–3. The following factors showed a significant difference between these groups of patients: GH/IGF-1 ratio, $P = 0.0009$; GH/IGFBP-3 ratio, $P = 0.0019$ (Fig. 2), but IGF-1/IGFBP-3 ratio did not have any statistical difference.

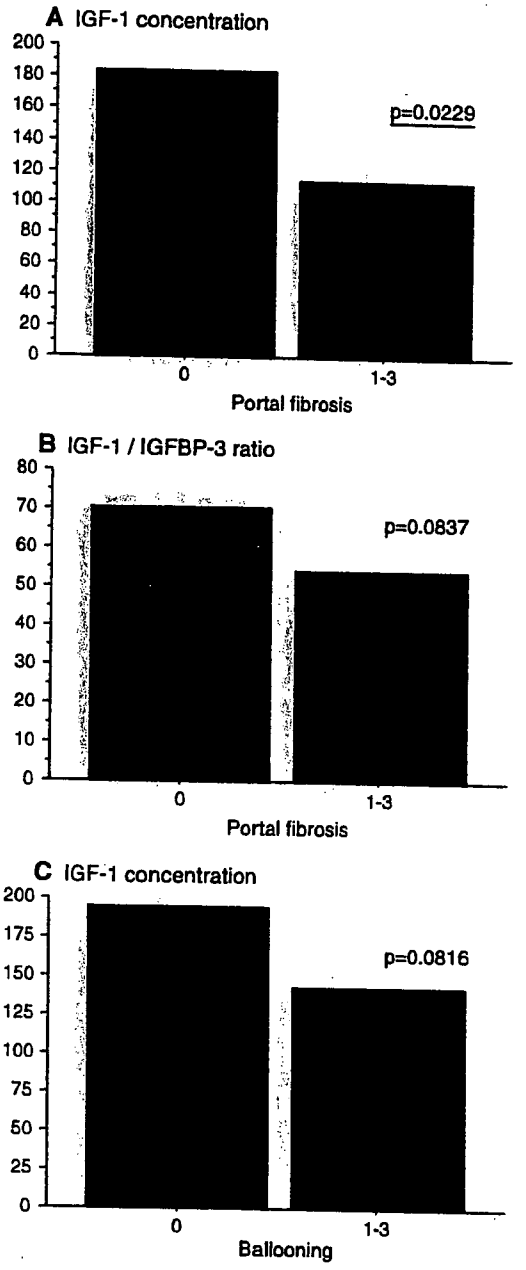

Fig. 1 Histopathologic factors and IGF-1: (A) relationship of portal fibrosis score and IGF-1 concentration (μg/l); (B) relationship of portal fibrosis score and IGF-1 concentration (μg/l)/IGFBP-3 concentration (mg/l) ratio; (C) relationship of ballooning score and IGF-1 concentration (μg/l). Statistical analysis by Mann–Whitney U test

Discussion

The data in this study shows that GH, IGF-1, and IGFBP-3 are predictors for the development of fibrosis and steatosis in NAFLD patients. Low levels of IGF-1 and IGF-1/IGFBP-3 may be associated with advanced fibrosis in NAFLD, and GH may be involved in the mechanism of

Table 4 Clinical and laboratory data for patients with steatosis of grade 1 and grades 2–3

Item	Steatosis 1 (n = 26)	Steatosis 2–3 (n = 26)	P-value
BMI	28.5 (4.48)	29.6 (3.75)	NS
Total cholesterol	193.7 (36.2)	211.4 (33.3)	0.034
Triglyceride	154.2 (65.6)	167.7 (66.6)	NS
GH	0.450 (0.458)	0.173 (0.162)	0.0236
IGF-1	157.1 (142.6)	184.3 (71.4)	0.0118
IGFBP-3	2.25 (0.58)	2.63 (0.68)	NS
Insulin	13.9 (5.89)	15.7 (7.83)	NS
Fasting plasma glucose	111.4 (28.2)	114.6 (38.2)	NS
HOMA-IR	4.02 (2.53)	4.04 (2.30)	NS
HbA1c	6.82 (1.75)	6.53 (2.08)	NS

Data are shown as means (standard deviation), with statistical analysis using a Mann–Whitney test

Table 5 Variables independently associated with steatosis of grade 2–3

Variable	Univariate analysis		Multivariate analysis	
	P-value	RR (95% CI)	P-value	RR (95% CI)
Total cholesterol	0.1239	2.424 (0.785–7.490)	0.3656	1.795 (0.506–6.372)
GH	0.0269	0.196 (0.046–0.830)	0.0414	0.199 (0.042–0.989)
IGF-1	0.0291	4.000 (1.151–13.901)	0.0676	3.628 (0.911–14.453)

The reference groups are total cholesterol > 200 mg/dl, GH > 0.3 ng/ml, and IGF-1 > 170 μg/l

triglyceride secretion from hepatocytes. It is of interest that our data are consistent with results of hormonal studies associated with atherosclerosis and metabolic syndrome [7, 9–11], and we speculate that the same hormonal profile results in development of hepatic steatosis and fibrosis in NAFLD, and that the mechanism of advanced fibrosis is common in development of atherosclerosis and visceral obesity.

Hepatic fibrosis is caused by activated hepatic stellate cells (HSC), which are activated by inflammatory cytokines in NAFLD [19]. Over expression of IGF-1 in HSC attenuates fibrogenesis and accelerates liver regeneration in a mouse model of CCl_4-induced liver damage [20]. These effects appear to be mediated in part by up-regulation of HGF and down-regulation of TGF-β1. Although GH is the major stimulant of IGF-1 synthesis in hepatocytes, inflammatory cytokines such as IL-1β [21], TNF-α [22] and IL-6 [23] inhibit IGF-1 secretion from hepatocytes. These cytokines are reported to have a pivotal role in development of NAFLD [24, 25], therefore, this may account for the decreased IGF-1 level and reduced IGF-1/IGFBP-3 ratio in advanced NASH and the negative correlation of these variables with the hyarulonic acid level. Based on the success of IGF-1 replacement therapy in animal models [26, 27], this therapy has recently been used for patients with liver cirrhosis [28]. IGF-1 supplementation protects the liver from damage, increases the albumin concentration and resting energy expenditure. The protective effects of IGF-1 on vascular cells, and endothelial function, atherosclerotic plaque development and ischemic myocardial damage all depend on nitric oxide production by activated PI3-k and Akt signaling in target cells [8]. IGF-1 induces glucose uptake in muscle [29] and low levels of IGF-1 produce different degrees of glucose tolerance in association with insulin sensitivity [30]; therefore, IGF-1 has been used successfully as an adjuvant to insulin therapy in patients with type 1 and 2 diabetes [29]. Insulin resistance is the most important factor in metabolic syndrome, including NAFLD and vascular disease, and low levels of IGF-1 may contribute to insulin resistance [29, 30]. IGF-1 has direct anti-fibrotic, cell protective and insulin-like actions and, decreases in IGF-1 and the IGF-1/IGFBP-3 ratio caused by inflammatory cytokines were associated with the development of advanced NAFLD, as well as serving as a marker for advanced NAFLD. In particular, our data show a tendency for low levels of IGF-1 and a low IGF-1/IGFBP-3 ratio in patients with portal fibrosis and ballooning. We speculate that this hormonal profile is required for progression of NAFLD, because of the emergence of portal fibrosis and ballooning in progressive NAFLD [31].

IGFBP-3 binds IGF-1 and an acid-labile subunit and forms a stable ternary complex, in which the half life of IGF-1 is prolonged and the bioactivity of IGF-1 is reduced [8]. New biological functions of IGFBP-3 have also been reported in recent years; for example, in mesangeal cells, IGFBP-3 mediates TNF-α and glucose-induced apoptosis by blocking Akt phosphorylation at threonine-308 [32].

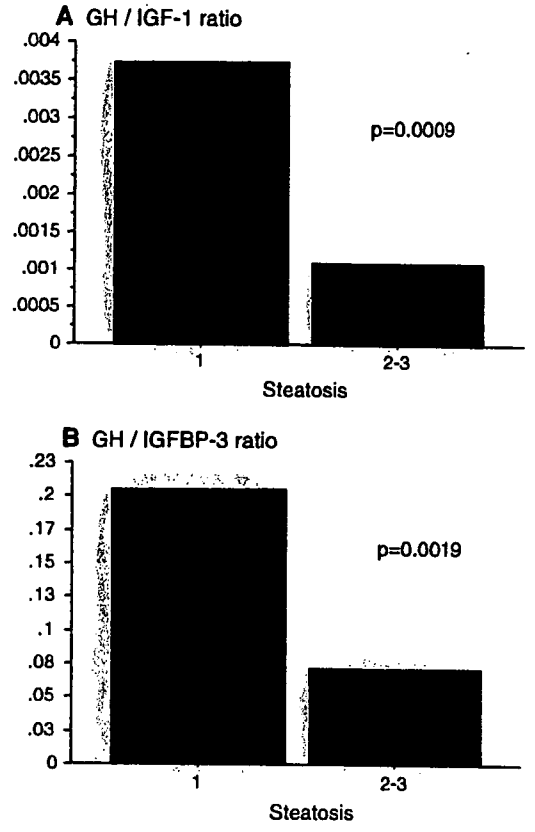

Fig. 2 Hepatic steatosis score and the GH axis: (**A**) relationship of steatosis score and GH (ng/ml)/IGF-1 concentration (μg/l) ratio; (**B**) relationship of steatosis score and GH (ng/ml)/IGFBP-1 concentration (mg/l) ratio. Statistical analysis by Mann–Whitney U test

Additionally, IGF-1 stimulates vascular endothelial growth factor (VEGF) and IGFBP-3 in retinal pigment epithelial cells, whereas, IGFBP-3 attenuates IGF-1-induced VEGF secretion [33]. IGF-1 also, inhibits TNF-α,(interferon γ and Fas-induced apoptosis in vascular smooth muscle cells, and TNF-α decreases IGF-1 and increases IGFBP-3 [22]. As stated above, IGFBP-3 binding reduces IGF-1 activity and the IGF-1/IGFBP-3 ratio therefore reflects the activity of IGF-1. In our study, hyaluronic acid, a hepatic fibrosis marker, showed negative correlations with IGF-1 ($r = -0.427$), IGFBP-3 ($r = -0.352$) and the IGF-1/IGFBP-3 ratio ($r = -0.436$). Although IGF-1 causes secretion of IGFBP-3 [6], we speculate that inflammatory cytokines decrease the levels of IGF-1 rather than those of IGFBP-3 in NAFLD patients, thereby decreasing the IGF-1/IGFBP-3 ratio. Therefore, a low IGF-1/IGFBP-3 ratio is a marker of advanced NAFLD, as it is for vascular disease.

The GH level did not show an association with fibrosis, but had a close affinity with steatosis in our cases. A low level of GH is the most reliable marker for advanced steatosis (grades 2–3], but the GH/IGF-1 and GH/IGFBP-3 ratios suggest that IGF-1 and IGFBP-3 are unrelated to steatosis. In previous reports, GH supplementation has been shown to reduce abdominal visceral fat in obese woman [34] and GHD patients [35], improve endothelial function in GHD patients [36], and decrease hepatic fat content in obese woman [34]. Such conditions are thought to promote GH-induced lipolysis in adipose tissue [37] and secretion of very low density lipoprotein from liver [38], and we suggest that low levels of GH may contribute to severe triglyceride accumulation in hepatocytes; though our results must be evaluated in a large cohort of patients.

In conclusion, GH, IGF-1 and IGFBP-3 are associated with fibrosis and steatosis of NAFLD. We speculate that a low level of IGF-1 and a low IGF-1/IGFBP-3 ratio may lead to development of fibrosis in NAFLD patients, whereas a low GH level contributes to development of hepatic steatosis. Since NAFLD is associated with metabolic syndrome, risk factors for development of these diseases show a common pattern of GH, IGF-1 and IGFBP-3 levels.

References

1. Johannsson G, Bengtsson BA. Growth hormone and the metabolic syndrome. J Endocrinol Invest 1999;22:41–6.
2. Ichikawa T, Hamasaki K, Ishikawa H, Ejima E, Eguchi K, Nakao K. Non-alcoholic steatohepatitis and hepatic steatosis in patients with adult onset growth hormone deficiency. Gut 2003;52:914.
3. Adams LA, Feldstein A, Lindor KD, Angulo P. Nonalcoholic fatty liver disease among patients with hypothalamic and pituitary dysfunction. Hepatology 2004;39:909–14.
4. Lonardo A, Loria P, Leonardi F, Ganazzi D, Carulli N. Growth hormone plasma levels in nonalcoholic fatty liver disease. Am J Gastroenterol 2002;97:1071–2.
5. Mauras N, Haymond MW. Are the metabolic effects of GH and IGF-I separable? Growth Horm IGF Res 2005;15:19–27.
6. Scharf J, Ramadori G, Braulke T, Hartmann H. Synthesis of insulin like growth factor binding proteins and of the acid-labile subunit in primary cultures of rat hepatocytes, of Kupffer cells, and in co-cultures: regulation by insulin, insulin like growth factor, and growth hormone. Hepatology 1996;23:818–27.
7. Juul A, Scheike T, Davidsen M, Gyllenborg J, Jorgensen T. Low serum insulin-like growth factor I is associated with increased risk of ischemic heart disease: a population-based case–control study. Circulation 2002;106:939–44.
8. Conti E, Carfozza C, Capoluongo E, Volpe M, Crea F, Zuppi C, Andreotti F. Insulin-like growth factor-1 as a vascular protective factor. Circulation 2004;110:2260–5.
9. Colao A, Spiezia S, Di Somma C, Pivonello R, Marzullo P, Rota F, Musella T, Auriemma RS, De Martino MC, Lombardi G. Circulating insulin-like growth factor-I levels are correlated with the atherosclerotic profile in healthy subjects independently of age. J Endocrinol Invest 2005;28:440–8.
10. Laughlin GA, Barrett-Connor E, Criqui MH, Kritz-Silverstein D. The prospective association of serum insulin-like growth factor I (IGF-I) and IGF-binding protein-1 levels with all cause and cardiovascular disease mortality in older adults: the Rancho Bernardo Study. J Clin Endocrinol Metab 2004;89:114–20.

11. Janssen JA, Stolk RP, Pols HA, Grobbee DE, Lamberts SW. Serum total IGF-I, free IGF-I, and IGFB-1 levels in an elderly population: relation to cardiovascular risk factors and disease. Arterioscler Thromb Vasc Biol 1998;18:277–82.
12. Adams LA, Lymp JF, St Sauver J, Sanderson SO, Lindor KD, Feldstein A, Angulo P. The natural history of nonalcoholic fatty liver disease: a population-based cohort study. Gastroenterology 2005;129:113–21.
13. Brea A, Mosquera D, Martin E, Arizti A, Cordero JL, Ros E. Nonalcoholic fatty liver disease is associated with carotid atherosclerosis: a case-control study. Arterioscler Thromb Vasc Biol 2005;25:1045–50.
14. Villanova N, Moscatiello S, Ramilli S, Bugianesi E, Magalotti D, Vanni E, Zoli M, Marchesini G. Endothelial dysfunction and cardiovascular risk profile in nonalcoholic fatty liver disease. Hepatology 2005;42:473–80.
15. Targher G. Associations between liver histology and early carotid atherosclerosis in subjects with nonalcoholic fatty liver disease. Hepatology 2005;42:974–5.
16. Brunt EM, Janney CG, Di Bisceglie AM, Neuschwander-Tetri BA, Bacon BR. Nonalcoholic steatohepatitis: a proposal for grading and staging the histological lesions. Am J Gastroenterol 1999;94:2467–74.
17. Taniguchi A, Fukushima M, Sakai M, Miwa K, Makita T, Nagata I, Nagasaka S, Doi K, Okumura T, Fukuda A, Kishimoto H, Fukuda T, Nakaishi S, Tokuyama K, Nakai Y. Remnant-like particle cholesterol, triglycerides, and insulin resistance in nonobese Japanese type 2 diabetic patients. Diabetes Care 2000;23:1766–9.
18. Zeng MD, Lu LG, Mao YM, Qiu DK, Li JQ, Wan MB, Chen CW, Wang JY, Cai X, Gao CF, Zhou XQ. Prediction of significant fibrosis in HBeAg-positive patients with chronic hepatitis B by a noninvasive model. Hepatology 2005;42:1437–45.
19. Elsharkawy AM, Oakley F, Mann DA. The role and regulation of hepatic stellate cell apoptosis in reversal of liver fibrosis. Apoptosis 2005;10:927–39.
20. Sanz S, Pucilowska JB, Liu S, Rodriguez-Ortigosa CM, Lund PK, Brenner DA, Fuller CR, Simmons JG, Pardo A, Martinez-Chantar ML, Fagin JA, Prieto J. Expression of insulin-like growth factor I by activated hepatic stellate cells reduces fibrogenesis and enhances regeneration after liver injury. Gut 2005;54:134–41.
21. Thissen JP, Verniers J. Inhibition by interleukin-1 beta and tumor necrosis factor-alpha of the insulin-like growth factor I messenger ribonucleic acid response to growth hormone in rat hepatocyte primary culture. Endocrinology 1997;138:1078–84.
22. Anwar A, Zahid AA, Scheidegger KJ, Brink M, Delafontaine P. Tumor necrosis factor-alpha regulates insulin-like growth factor-1 and insulin-like growth factor binding protein-3 expression in vascular smooth muscle. Circulation 2002;105:1220–5.
23. Lelbach A, Scharf JG, Ramadori G. Regulation of insulin-like growth factor-I and of insulin-like growth factor binding protein-1, -3 and -4 in cocultures of rat hepatocytes and Kupffer cells by interleukin-6. J Hepatol 2001;35:558–67.
24. Nozaki Y, Saibara T, Nemoto Y, Ono M, Akisawa N, Iwasaki S, Hayashi Y, Hiroi M, Enzan H, Onishi S. Polymorphisms of interleukin-1 beta and beta 3-adrenergic receptor in Japanese patients with nonalcoholic steatohepatitis. Alcohol Clin Exp Res 2004;28:106S–10S.
25. Larter CZ, Farrell GC. Insulin resistance, adiponectin, cytokines in NASH: which is the best target to treat? J Hepatol 2006;44:253–61.
26. Castilla-Cortazar I, Garcia M, Muguerza B, Quiroga J, Perez R, Santidrian S, Prieto J. Hepatoprotective effects of insulin-like growth factor I in rats with carbon tetrachloride-induced cirrhosis. Gastroenterology 1997;113:1682–91.
27. Garcia-Fernandez M, Castilla-Cortazar I, Diaz-Sanchez M, Navarro I, Puche JE, Castilla A, Casares AD, Clavijo E, Gonzalez-Baron S. Antioxidant effects of insulin-like growth factor-I (IGF-I) in rats with advanced liver cirrhosis. BMC Gastroenterol 2005;5:7.
28. Conchillo M, de Knegt RJ, Payeras M, Quiroga J, Sangro B, Herrero JI, Castilla-Cortazar I, Frystyk J, Flyvbjerg A, Yoshizawa C, Jansen PL, Scharschmidt B, Prieto J. Insulin-like growth factor I (IGF-I) replacement therapy increases albumin concentration in liver cirrhosis: results of a pilot randomized controlled clinical trial. J Hepatol 2005;43:630–6.
29. Dominici FP, Argentino DP, Munoz MC, Miquet JG, Sotelo AI, Turyn D. Influence of the crosstalk between growth hormone and insulin signalling on the modulation of insulin sensitivity. Growth Horm IGF Res 2005;15:324–36.
30. Sesti G, Sciacqua A, Cardellini M, Marini MA, Maio R, Vatrano M, Succurro E, Lauro R, Federici M, Perticone F. Plasma concentration of IGF-I is independently associated with insulin sensitivity in subjects with different degrees of glucose tolerance. Diabetes Care 2005;28:120–5.
31. Morita Y, Ueno T, Sasaki N, Kuhara K, Yoshioka S, Tateishi Y, Nagata E, Kage M, Sata M. Comparison of liver histology between patients with non-alcoholic steatohepatitis and patients with alcoholic steatohepatitis in Japan. Alcohol Clin Exp Res 2005;29:277S–81S.
32. Vasylyeva TL, Chen X, Ferry RJ Jr. Insulin-like growth factor binding protein-3 mediates cytokine-induced mesangial cell apoptosis. Growth Horm IGF Res 2005;15:207–14.
33. Slomiany MG, Rosenzweig SA. Autocrine effects of IGF-I-induced VEGF and IGFBP-3 secretion in retinal pigment epithelial cell line ARPE-19. Am J Physiol Cell Physiol 2004; 287:C746–53.
34. Franco C, Brandberg J, Lonn L, Andersson B, Bengtsson BA, Johannsson G. Growth hormone treatment reduces abdominal visceral fat in postmenopausal women with abdominal obesity: a 12-month placebo-controlled trial. J Clin Endocrinol Metab 2005;90:1466–74.
35. Eden Engstrom B, Burman P, Holdstock C, Karlsson FA. Effects of growth hormone (GH) on ghrelin, leptin, and adiponectin in GH-deficient patients. J Clin Endocrinol Metab 2003;88:5193–8.
36. Abdu TA, Elhadd TA, Buch H, Barton D, Neary R, Clayton RN. Recombinant GH replacement in hypopituitary adults improves endothelial cell function and reduces calculated absolute and relative coronary risk. Clin Endocrinol (Oxf) 2004;61:387–93.
37. Kersten S. Mechanisms of nutritional and hormonal regulation of lipogenesis. EMBO Rep 2001;2:282–6.
38. Frick F, Linden D, Ameen C, Eden S, Mode A, Oscarsson J. Interaction between growth hormone and insulin in the regulation of lipoprotein metabolism in the rat. Am J Physiol Endocrinol Metab 2002;283:E1023–31.

ELSEVIER

Cerebellar Ataxia in a Patient Receiving Calcineurin Inhibitors After Living Donor Liver Transplantation: A Case Report

I. Yamaguchi, T. Ichikawa, K. Nakao, K. Hamasaki, K. Hirano, S. Eguchi, M. Takatsuki, Y. Kawasita, T. Kanematsu, and K. Eguchi

ABSTRACT

Neurological complications of calcineurin inhibitors are frequent problems after transplantation. Cerebellar ataxia with other neurological findings and an abnormal density area in the subcortical white matter are found by MRI in the brains of most patients with central nervous system complications caused by calcineurin inhibitors. Such neurological complications are not life-threatening, but have a negative impact on the quality of life. We describe a 58-year-old woman who developed cerebellar ataxia at 4 days after living donor liver transplantation. She walked with a swaying gait, and after walking for 5 minutes she was unable to stand. Her symptoms persisted after a change from tacrolimus to cyclosporine, but dose reduction of cyclosporine and addition of mycophenolate mofetil cured the ataxia. We diagnosed a case of cerebellar ataxia without leukoencephalopathy or other neurological symptoms, as a new complication of calcineurin inhibitor treatment. We concluded that careful attention should be paid to neurological complications of calcineurin inhibitors.

TACROLIMUS (Tac) and cyclosporine (CsA) are calcineurin inhibitors that have powerful immunosuppressant actions, which may lead to adverse neurological effects postoperatively in organ transplant patients. In a previous report,[1] calcineurin inhibitors were shown to cause various neurotoxic events, including seizures, tremors, changes in mental state, peripheral neuropathy, and leukoencephalopathy among 10% to 28% of treated patients. Most patients suffered leukoencephalopathy. Herein, we have reported a case of a patient who received a living donor liver transplantation (LDLT) and subsequently developed cerebellar ataxia which manifested as gait and speech disturbances. This complication resolved following reduction of the calcineurin inhibitor dose. This case differs from previously reported cases regarding neurological symptoms and brain MRI findings.

CASE REPORT

A 58-year-old woman with hepatitis C virus (HCV; genotype 1b and 2140 fmol/L serum core protein) and decompensated liver cirrhosis underwent LDLT. Before LDLT, she had experienced hepatic encephalopathy, but did not have any other neurological complication. After LDLT, Tac and prednisone were administered at the standard doses used in our immunosuppressive protocol. On postoperative day (POD) 7, she had slurred speech and intention tremor, but these occurred without seizure, muscle weakness, or any other neurological symptoms except for cerebellar ataxia. Her gait posture had a wide base, she swayed while walking, and she could barely walk for 5 minutes before becoming unstable. She could not stand on one foot and or step in tandem gait. We thought that her neurological condition was due to cerebellar ataxia caused by Tac.

On POD 23, laboratory data showed 1100 fmol/L HCV virus titer, 754 IU/mL alanine aminotransferase (ALT) 853 IU/mL alkaline phosphatase (ALP), and 3.0 mg/dL total bilirubin. We diagnosed reactivation of HCV based on the laboratory data and a liver biopsy, and started interferon (IFN) α-2b at 3 million units subcutaneously 3 times per week plus ribavirin (Rib) at 400 mg/d orally for 24 weeks. Because of the persistence of her neurological symptoms, Tac was discontinued and CsA was started from POD 22. At the end of the IFN plus Rib therapy, HCV remained in her serum. Therefore, she resumed pegylated IFN (peg-IFN) α-2b (60 μg subcutaneously once per week) plus Rib (600 mg/d orally for 24 weeks) from postoperative week 38. Within the period of peg-IFN α-2b plus Rib treatment, the serum HCV virus titer decreased but

From the First Department of Internal Medicine (I.Y., T.I., K.N., K.H., K.E.) and Departments of Clinical pharmaceutics (K.H.) and Transplantation and Digestive Surgery (S.E., M.T., Y.K., T.K.), Graduate School of Biomedical Science, Nagasaki University, Nagasaki, Japan.

Address reprint requests to Tatsuki Ichikawa, MD, First Department of Internal Medicine, Graduate School of Biomedical Science, Nagasaki University, 1-7-1 Sakamoto, Nagasaki, Japan. E-mail: ichikawa@net.nagasaki-u.ac.jp

0041-1345/07/$–see front matter
doi:10.1016/j.transproceed.2007.08.092

her laboratory data did not normalize and she experienced an auditory disturbance in her right ear due to adverse effects of IFN treatment. On MRI on POD 48, no abnormal intensity regions were found in the deep white matter in the cerebrum and cerebellum. Because cerebellar ataxia persisted after the change from Tac to CsA, she tended to fall down easily and her independent range of movement was restricted. At postoperative month 13, peg-IFN α-2b plus Rib therapy was terminated at the cutoff date for this therapy. After cessation of IFN combination therapy, her laboratory data worsened and the serum HCV virus titer was elevated. The hearing disturbance subsided, but the neurological symptoms due to cerebellar ataxia continued. We determined that retreatment with IFN plus Rib was needed to repress liver fibrosis. On POD 464, the patient undertook a new immunosuppressive regimen including CsA, which was reduced from 200 to 100 mg/d, and mycophenolate mofetil (MMF), 1 g/d. The next day, cerebellar ataxia improved and she could walk for 20 minutes or more. The blood CsA concentration fell below therapeutic range, 48 ng/mL, after reduction of the CsA dose. Two months after reduction of CsA, the patient was not conscious of cerebellar ataxia, since her independent activities were no longer restricted, and she did not have intention tremor, or the inability to step in tandem gait or stand on one foot. In this context, peg-IFN α2a (180 μg once per week) and Rib (400 mg daily for 48 weeks) had been started from POD 452, and the HCV titer decreased from 71,400 fmol/L to below the detection limit in the HCV core protein assay. Similarly, ALT decreased from 192 to 50 IU/mL in the 2 months after the start of the new anti-HCV regimen. Follow-up brain MRI was performed at the termination of the new anti-HCV regimen; no abnormal intensity area was found in the brain. The patient no longer noticed hearing disturbances during this period, despite the repeated IFN treatment.

DISCUSSION

Liver transplantation is now a well-established treatment for end-stage liver disease. The quality of life after liver transplantation is excellent in most patients, but some patients suffer complications, many of which are related to the immunosuppressive therapy.[2] Neurological complications are common adverse effects of immunosuppressants, and calcineurin inhibitors are known for their neurotoxicity. The majority of neurological complications are not life-threatening,[3] but lead to an impaired quality of life. In our case, cerebellar ataxia decreased the activities of our patient, and a calcineurin inhibitor sparing regimen improved her lifestyle following amelioration of cerebellar ataxia. Our experience suggested that greater consideration of neurological complications caused by adverse effects of calcineurin inhibitors is warranted, because impaired quality of life caused by postoperative neurological complications can be improved by dose reduction of calcineurin inhibitors.[1]

In most cases, central nervous system complications caused by CsA involve lesions with increased signal intensity on MRI T2-weighted images, with these lesions affecting the subcortical white matter.[4] In other reports, cerebrocerebellar syndrome,[3] cerebellar syndrome,[5] mutism with ataxia,[6] loss of speech with ataxia,[7] and late-onset ataxia[8] have been associated with high signal intensity regions in the white matter on MRI T2-weighted images. Such high signal intensity in the white matter on MRI is referred to as leukoencephalopathy, a well-known clinical aspect of various types of toxic encephalopathy, including that due to calcineurin inhibitors.[9] In contrast, ataxia without abnormal MRI findings represents a rare form of neurological complication following liver transplantation.[3] Leukoencephalopathy was not found in the subcortical white matter in our case, but we consider that the case was still a toxic complication of a calcineurin inhibitor, because of the improved ataxia upon reduction of the CsA dose. Therefore, we assume that the neurological complications were also adverse effects of the calcineurin inhibitor, despite the absence of MRI findings. The mechanisms of neurological toxicity without leukoencephalopathy are not well understood. In vitro experiments[1] have shown that Tac and CsA have selective toxicity for glial cells and induce apoptosis of oligodendrocytes. It is speculated that these events correlate with typical white matter changes. However, Tac and CsA may modulate the activity of amino acid receptors via calcineurin in neurons.[1] This phenomenon may cause alteration of neuronal function and development of neurological complications without morphological changes in the brain. Hence, it is possible that a patient with neurological complications caused by calcineurin inhibitors could show normal deep white matter on MRI.

Although the neurological symptoms in our case were of the early-onset posttransplantation type, as in other reports,[1] ataxia without other neurological symptoms is rare in a patient receiving a calcineurin inhibitor. Previously reported patients with neurological complications who were treated with Tac and CsA almost always had ataxia plus other neurological symptoms, such as muscle weakness[7] or blindness and seizure.[3] Ataxia alone has been reported in a late-onset case of neurological complications induced by a calcineurin inhibitor,[10] and the cerebellum has been reported to be affected in a few cases.[11] However, the mechanism of cerebellum neurotoxicity remains unknown, and it is more likely that the cerebellar hemisphere alone is damaged by calcineurin inhibitors. Calcineurin plays a pivotal role in cerebellar development,[12] and the calcineurin signal may contribute to the maturation and refinement of cerebellar circuit formation.[12] Therefore, we suggest that a calcineurin inhibitor can have a functional influence on the cerebellum without causing morphological changes.

Central nervous system involvement in HCV infection with or without cryoglobulinemia has been reported previously.[13] Therefore, it is a key issue whether calcineurin inhibitors were more relevant to the neurological symptoms of this case rather than reactivation of HCV infection after LDLT. As described in the clinical course, HCV activity decreased during the therapy with IFN or peg-IFN plus Rib and increased after cessation of therapy. Cerebellar ataxia persisted independently of HCV activity, but improved after dose reduction of CsA. Taken together, it is possible that calcineurin inhibitors rather than HCV activity were